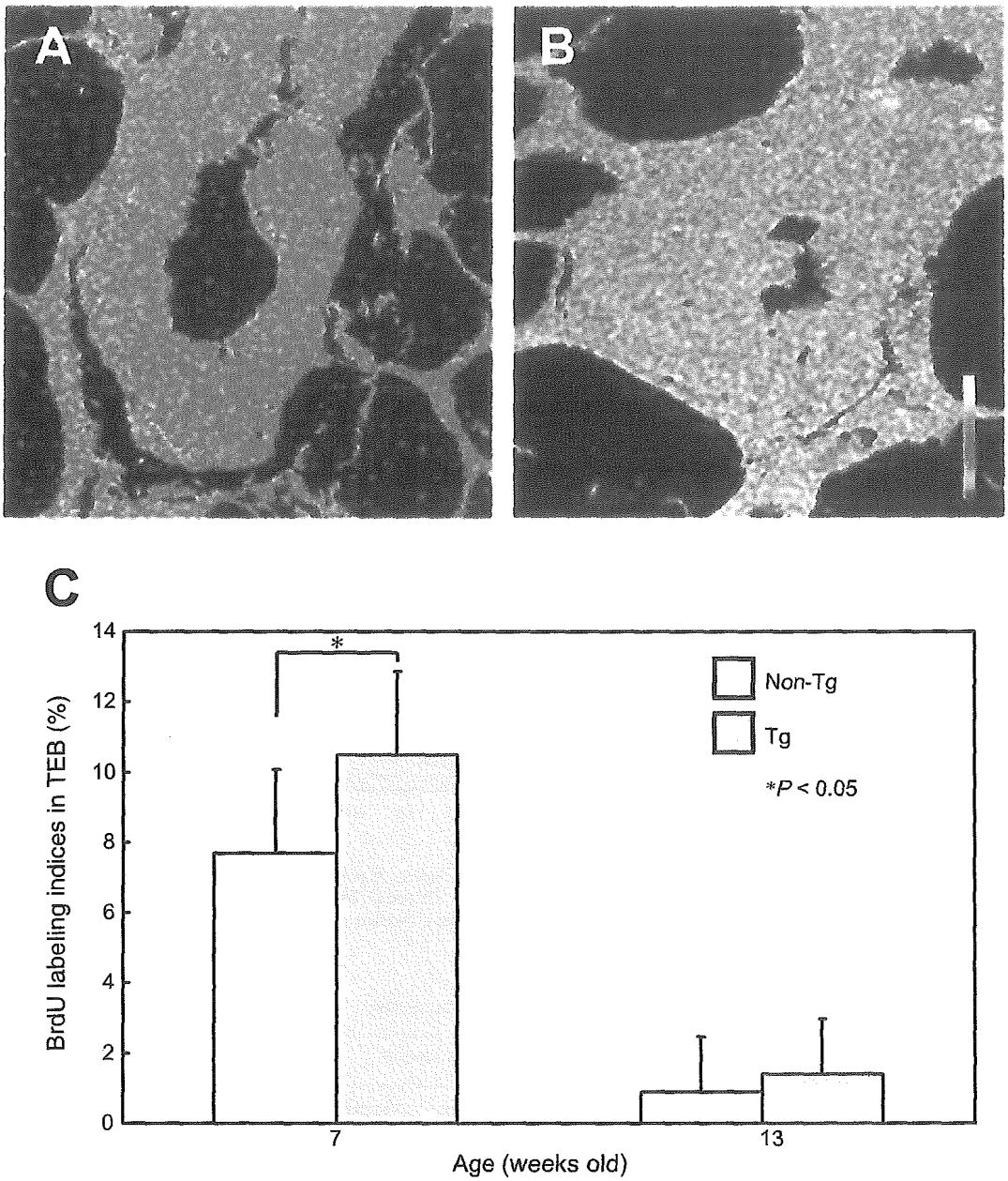

Figure 2. Higher levels of active MAPK and cell proliferation in TEBs of transgenic rats. Pseudocolor displays of phosphoMAPK/MAPK ratios in the TEBs of 49-day-old non-transgenic (A) and transgenic (B) rats. (C) BrdU labeling indices in TEBs of non-Tg and Tg rats at the indicated time points.

(BrdU) (Wako Pure Chemical, Osaka, Japan) 1 h before sacrifice. Tissue sections were deparaffinized and rehydrated according to standard protocols, incubated in 1 N HCl for 20 min and in 0.01% actinase E (Kaken Pharmaceutical Co., Ltd., Tokyo, Japan) in PBS for 5 min at 37°C and then blocked with 1% skim milk in PBS for 1 h. Mouse monoclonal anti-BrdU antibody (1:200 dilution) (Beckton Dickinson, Franklin Lakes, NJ) was applied overnight at 4°C, and immunocomplexes were visualized using a Vectastain ABC kit (Vecton Laboratories, Burlingame, CA) according to the manufacturer's protocol. Labeling indices were

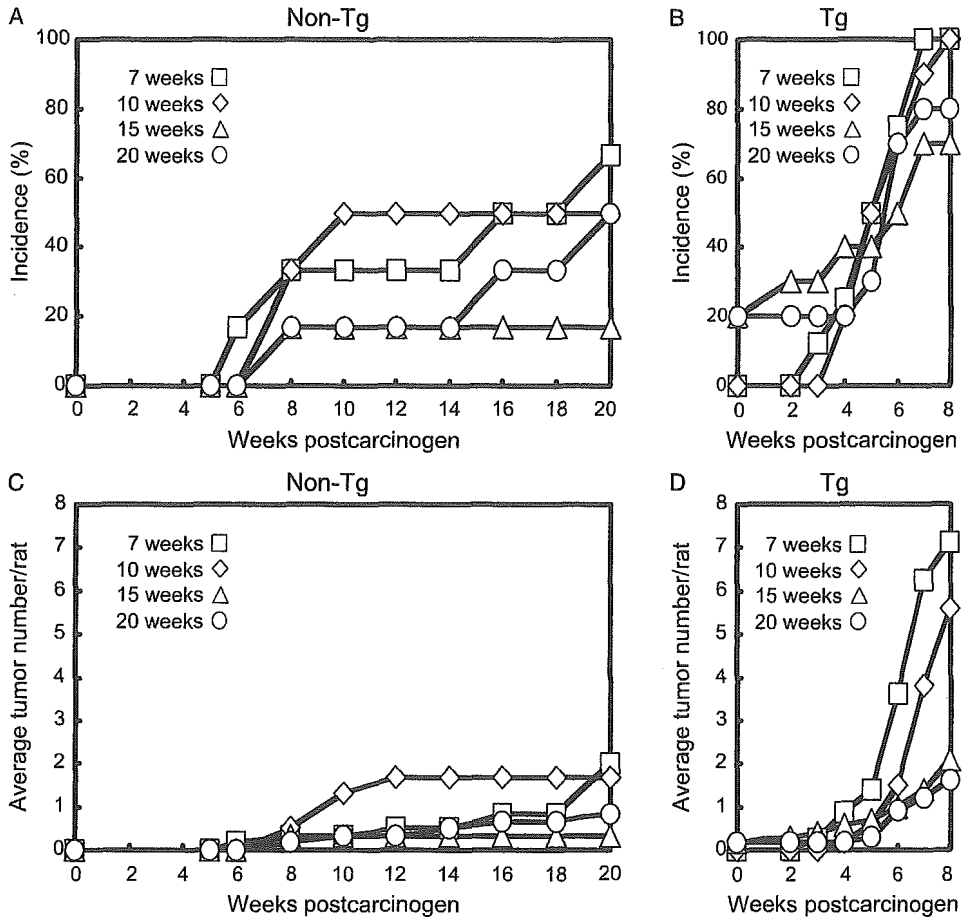

Figure 3. Relationship between age of administration of DMBA and induction of palpable mammary tumors. Rats were given a single i.g. injection of DMBA at 7 (□), 10 (◇), 15 (△) or 20 (○) weeks old of age. (A and B) Incidence of palpable mammary tumors as a function of time after the treatment. (C and D) Average number of the tumors per rat as a function of time after the treatment.

Table 1. Incidences and number of tumors in DMBA-treated non-Tg rats at sacrifice

Age DMBA injected (weeks)	Number of rats	Atypical hyperplasia		Adenocarcinoma		Total		Weight of tumors (mean ± SD)
		Incidence (%)	No./rats (mean ± SD)	Incidence (%)	No./rats (mean ± SD)	Incidence (%)	No./rats (mean ± SD)	
7	6	0 (0)	0	5 (83.3)	4.7 ± 4.0	5 (83.3)	4.7 ± 4.0	3.33 ± 5.58
10	6	1 (16.7)	0.3 ± 0.8	4 (66.7)	2.0 ± 2.1	3 (66.7)	2.3 ± 2.6	3.26 ± 6.83
15	6	1 (16.7)	0.2 ± 0.4	1 (16.7)	0.2 ± 0.4[a]	2 (33.3)	0.3 ± 0.5[a]	0.01 ± 0.01
20	6	0 (0)	0	3 (50)	0.8 ± 1.2[b]	3 (50)	0.8 ± 1.2[b]	1.03 ± 1.55

[a] $P < 0.01$ as compared to 7-week-old-rats.
[b] $P < 0.05$ as compared to 7-week-old-rats.

calculated for nine TEBs. In some experiments, immunostaining with monoclonal anti-PCNA antibody (Dako Japan, Kyoto, Japan) was carried out after autoclaving sections for 15 min at 121°C. At least three ductal structures per rat were counted for cell proliferation analysis, representing a total of 500–1000 cells.

Table 2. Incidences and number of tumors in DMBA-treated Tg rats at sacrifice

Age DMBA injected (weeks)	Number of rats	Atypical hyperplasia		Adenocarcinoma		Total		Weight of tumors (mean ± SD)
		Incidence (%)	No./rats (mean ± SD)	Incidence (%)	No./rats (mean ± SD)	Incidence (%)	No./rats (mean ± SD)	
7	8	0 (0)	0	8 (80)	11.3 ± 7.1	8 (100)	11.3 ± 7.1	6.70 ± 9.03
10	10	0 (0)	0	10 (100)	7.5 ± 4.8	10 (100)	7.5 ± 4.8	2.92 ± 2.38
15	10	0 (0)	0	8 (80)	4.6 ± 5.3[a]	8 (80)	4.6 ± 5.3[a]	4.73 ± 6.42
20	10	0 (0)	0	8 (80)	3.6 ± 3.3[b]	8 (80)	3.6 ± 3.3[b]	5.69 ± 7.60

[a] $P < 0.05$ as compared to 7-week-old-rats.
[b] $P < 0.01$ as compared to 7-week-old-rats.

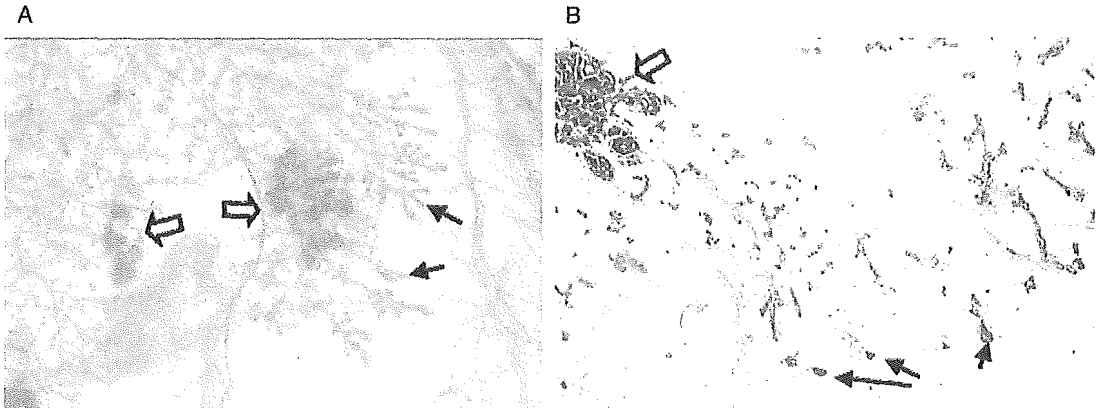

Figure 4. Representative whole mount and histological preparations of abdominal mammary glands at 20 days after treatment with MNU. (A) The whole mount was stained with alum carmine as described in the Materials and methods. (B) An early adenocarcinoma is located in close proximity to TEBs with normal morphology. Open arrows indicate neoplastic lesions and closed arrows indicate TEBs. The magnification of photomicrograph is 50×.

Restriction fragment length polymorphisms (RFLPs)

Three to five TEBs or neoplastic lesions from each row of mammary glands were carefully scraped out of paraffin sections with scalpels, and DNA was extracted using Takara DEXPAT (Takara Biomedicals, Ohtsu, Japan). RFLP analyses of codons 12 and 61 of the human c-Ha-ras transgene were carried out as described previously [12] with minor modifications. In brief, 165 bp fragments of codon 12 were first amplified with specific primers for the human gene (forward, 5′-GGACCCCGGGCCGCAGGCCCC-3′, reverse, 5′-CCTGGACGGCGGCGCTAGG-3′) with an annealing step for 30 s at 60°C and extension for 30 s at 72°C for 20 cycles. Second round PCR using a 1:50 diluent of the first PCR products as the template and the same primer set was performed for 25 cycles under the same conditions. *Msp*I digestion of wild type ras gave 103 and 62 bp fragments. For the first round PCR of codon 61, forward; 5′-CTGTGTGAACTCCCCCCACGGA-3′ and reverse; 5′-AAAGCGAGAGCTGGCTACGGG-3′ primers were used. The subsequent procedures were the same as described previously [12].

RT-PCR

First-strand cDNA synthesis from total RNA and PCR amplifications using the following primers were performed as described elsewhere [34]: human and rat c-Ha-ras, forward, 5′-CCAGCTGATCCAGAACCATT-3′, reverse, 5′-AGCACACACTTGCAGCTCAT-3′; cyclin D1, forward, 5′-AGCTCCTGTGCTGCGAAG TG-3′, reverse, 5′-TCAGATGTCCACATCTCGGAC-3′; cyclin D2, forward, 5′-CCGCAACCTGCTGGAA GACC-3′, reverse, 5′-TCACAGGTCAACATCCCGC AC-3′; cyclin D3, forward, 5′-CCTGCAGAGTTTGC TCCGCT-3′, reverse, 5′-CTACAGGTGGATGGCTG

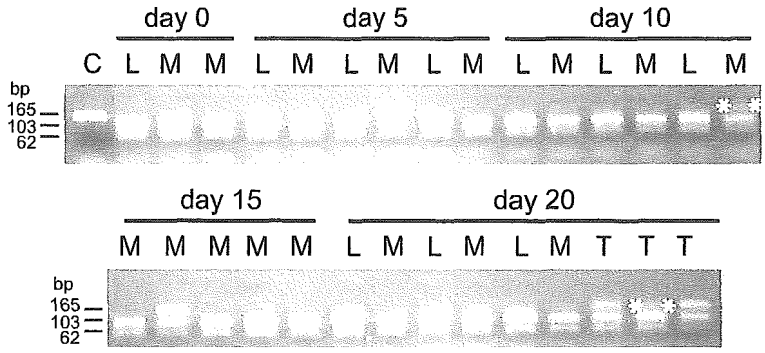

Figure 5. Elevated expression of c-Ha-ras genes in transgenic mammary glands and ras mutations in alveolar hyperplastic nodules. Representative RFLP analysis data of codon 12 of the human c-Ha-ras gene in TEBs after a single injection of MNU into Tg rats. DNA samples were collected from single TEBs of 3–5 individual Tg rats at each time point. C, control cDNA of human c-Ha-ras with a mutation in codon 12; L, liver DNA from each corresponding Tg rat of which TEB DNA was collected; M, DNA from a single TEB with normal morphology in the mammary gland; T, tumor DNAs from three individual Tg rats. Asterisks indicate faint 165 bp bands corresponding to mutant ras.

TGAC-3′; GAPDH, forward, 5′-TTCAACGGCACAG TCAAGG-3′, reverse, 5′-CATGGACTGTGGTCAT GAG-3′.

Fluorescence in situ *hybridization (FISH)*

Chromosome slides for FISH were prepared according the procedure described previously [35]. Lymphocytes were isolated from the spleens of female transgenic rats (9 weeks old), washed twice with serum-free RPMI1640 medium, and transferred to 25 cm^2 culture flasks containing 10 ml of RPMI1640 supplemented with 20% FCS, 3 μg/ml concanavalin A (Type IV-S, Sigma, St. Louis, MO), 10 μg/ml lipopolysaccharide (Sigma, St. Louis, MO) and 5×10^{-5} M-mercaptoethanol (Sigma, St. Louis, MO). Culture with 0.5×10^6 cells/ml were incubated in a humidified atmosphere of 5% CO_2 in air for 45 h, then treated with colcemid (0.02 μg/ml) for an additional 30 min. Cell suspensions were then collected, treated with 0.075 M KCl, fixed with 3:1 methanol: glacial acetic acid, and air-dried. The chromosome slides were hardened at 65°C for 4 h, treated with 30 μg/ml pepsin (Sigma, St. Louis, MO) for 5 min, washed twice with PBS for 5 min, PBS/50 mM $MgCl_2$ for 5 min, 1% formalin/50 mM $MgCl_2$/PBS for 10 min, PBS for 5 min, and dehydrated through a 70, 80, and 100% ethanol series for 3 min each. They were then denaturated at 70°C for 2 min in 70% formamide in 2× SSC. A 6.8 kb of *Bam*HI-digested genomic fragment of the human c-Ha-ras was labeled with a nick translation kit using biotin 16-dUTP (Roche Molecular Biochemicals, Mannheim, Germany) according to the manufacturer's protocol. The labeled probe was ethanol-precipitated with salmon sperm DNA and tRNA, denatured in 100% formamide for 10 min at 75° C, and mixed with an equal volume of hybridization solution to a final concentration of 50% formamide, 2× SSC, 10% dextran sulfate and 1 mg/ml BSA. The slides were then incubated with 300 ng of the probe overnight, and washed in 50% formamide/2× SSC for 20 min followed by 2× SSC and 1× SSC for 20 min each at room temperature. After rinsing in 4× SSC, they were incubated with FITC-avidin (Vector Laboratories, Burlingame, CA) in 10% Block Ace (Dainippon Pharmaceutical Co. Ltd., Osaka, Japan) for 1 h, then washed with 4× SSC, 0.1% Triton X-100/4× SSC, and 4× SSC for 10 min each. After draining the excess liquid from the slides, DNA was stained with 4′,6-diamidino-2-phenylindole

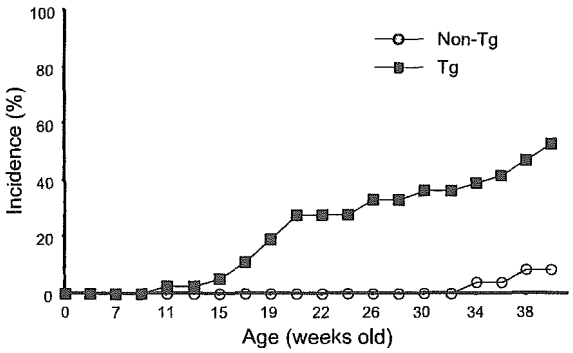

Figure 6. Incidences of spontaneous mammary tumors in non-Tg and Tg rats. The total number of non-Tg and Tg animals under examination were 24 and 36, respectively. Non-Tg, non-transgenic littermates; Tg, human c-Ha-ras transgenic rats.

dihydrochloride *n*-hydrate in VECTASHIELD Mounting Medium (Vector Laboratories, Burlingame, CA). All procedures were carried out at 37°C unless otherwise stated.

Results

Analyses of mammary glands during sexual maturation

Whole mount preparations were used to compare the appearance of the mammary glands of transgenic (Tg) virgin females with that of non-Tg virgin females during postnatal mammary development (Figure 1(A)). While the ductal shape, branching pattern, and direction of ductal growth in Tg mammary glands were indistinguishable from those of non-Tg glands until 49 days, Tg glands appeared to fill a greater area of the fat pad than non-Tg glands at 63 days after birth (Figure 1(A)).

We counted number of TEBs in the abdominal mammary glands of 49 to 91-day-old female non-Tg and Tg rats and found the numbers to be significantly ($P < 0.05$) higher in Tg rats until 81 days (Figure 1(B)). At 63 and 70 days, there were more than twice as many TEBs in Tg as in non-Tg rats. However, there was no difference in the rates of decrease in number of TEBs (TEB decrease/day) over time. The results thus suggest an earlier onset and/or higher rate of ductal cell proliferation in Tg mammary glands rather than a decreased rate of cell differentiation.

Since activation of the ras-MAPK cascade leads to cell proliferation, we employed confocal microscopy to measure the level of phosphorylation, that is, activation, of MAPK in TEBs (Figure 2(A) and (B)). The mean phosphoMAPK/MAPK ratios in 49-day-old non-Tg (Figure 2(A)) and Tg (Figure 2(B)) TEBs were 1.13 ± 0.13 ($n = 5$) and 1.40 ± 0.22 ($n = 5$), respectively, indicating that more MAPK was in the active state in the Tg TEBs. It is noteworthy that the ratio was also higher in Tg stroma than in non-Tg stroma surrounding TEBs (Figure 2(A) and (B)). The bromodeoxyuridine-labeling indices of 49-day-old non-Tg and Tg TEBs were $7.7 \pm 2.0\%$ ($n = 9$) and $10.5 \pm 2.4\%$ ($n = 6$), respectively, further confirming a significantly ($P < 0.05$) higher growth rate of Tg TEBs during sexual maturation (Figure 2(C)).

Relationship between TEB numbers and tumorigenic response initiated by chemical carcinogen in Tg rats

Non-Tg rats developed palpable mammary tumors at the highest incidence when they were inoculated with DMBA at 7 weeks of age and showed a tendency for a decrease in incidence with age at initiation (Figure 3(A)), as reported previously [1, 6]. Although no significant differences in the incidence and the mean weight of mammary tumors were noted among the four age groups at autopsy, significantly fewer adenocarcinomas per animal were observed during the experimental period in the groups receiving DMBA at 15 and 20 weeks of age compared to 7-week-old animals (Figure 3(C) and Table 1). All of the Tg rats inoculated with DMBA at 7 weeks of age rapidly developed palpable tumors within 8 weeks as demonstrated previously [31], and more than 70% of those initiated at 10, 15 or 20 weeks of age developed tumors as well (Figure 3(B)). There were no significant differences in the incidence and the mean weight of mammary tumors among the four groups of Tg rats at autopsy (Table 2). However, Tg rats inoculated at 15 and 20 weeks of age showed significantly fewer adenocarcinomas per animal, 4.6 ± 5.3 and 3.6 ± 3.3, respectively, compared with those inoculated at 7 weeks of age (Figure 3(D) and Table 2). This result is consistent with the conclusion that the TEB is the major target of chemical carcinogens in rat mammary glands.

Early neoplastic lesions in mammary ducts are located in close proximity to TEBs

We have recently reported that almost all Tg rats develop proliferative intraductal lesions by 20 days after MNU injection as shown in Figure 4(A) [30]. Most of the lesions were found to be located in close proximity to TEBs (closed arrows in Figure 4) suggesting that they originated from previous TEBs. Histological analysis revealed these lesions to be atypical hyperplasias and adenocarcinomas (Figure 4(B)) as reported previously [30].

TEBs are targets of a direct-acting chemical carcinogen

The human c-Ha-ras transgene was here utilized as a probe to monitor ras mutations because of its higher mutation rate compared to the rat endogenous

gene [12]. Restriction fragment length polymorphism (RFLP) analysis revealed that TEB samples of Tg rats sacrificed at 5, 10 and 15 days after MNU injection, when adenocarcinomas were rare [30], already harbored mutations in codon 12 of the human c-Ha-ras gene (Figure 5). This result reinforces the evidence for TEBs being targets of chemical carcinogens. Interestingly, no mutation was detectable in the samples obtained from TEBs with normal morphology at 20 days after MNU inoculation although all of the adenocarcinomas developed in each rat harbored ras mutations (Figure 5). By contrast, RFLP analysis detected mutations neither at codon 61 of human c-Ha-ras gene in any of the TEBs and tumor samples (data not shown), nor at codons 12 and 61 in the liver (Figure 5, data not shown). Based on all of the above findings taken together, we conclude that TEBs are one of the major targets of chemical carcinogens in the mammary glands of Tg rats.

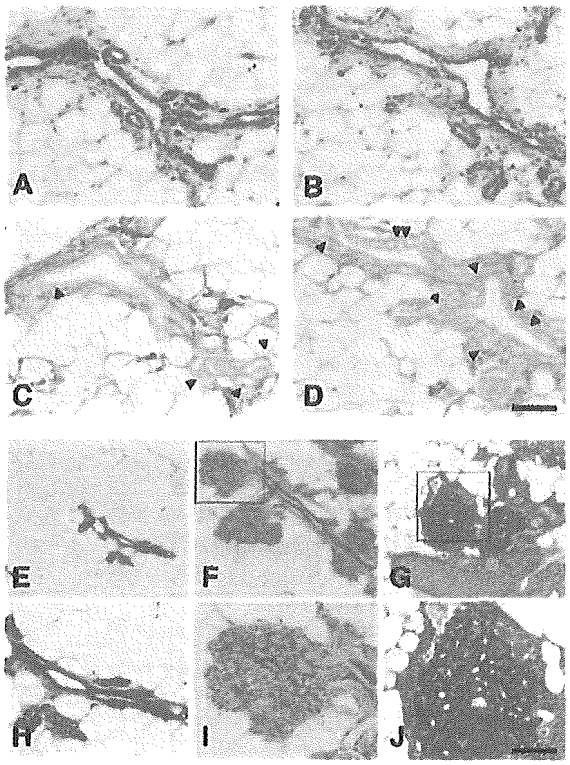

Figure 7. Highly proliferative ductal epithelium and development of alveolar hyperplasia in aged c-Ha-ras transgenic rats. At 70 days of age (A–D), the number of PCNA-positive nuclei (arrowheads) in the ductal epithelium of Tg rats (D) was significantly higher than in the ductal epithelium of non-transgenic rats (C). Panels A and B correspond to the HE-stained sections of panels C and D, respectively. Mammary glands of 35-week-old non-transgenic (E and H) and transgenic (F, G, I and J) rats. Alveolar hyperplastic nodules without (F and I) or with (G and J) cellular atypia were observed in all transgenic rats. Panels H, I, and J are higher magnification images of panels E, F, and G, respectively. Bars: 100 μm for A–D, H–J; 250 μm for E–G.

Incidence of sporadic mammary tumors in c-Ha-ras Tg rats

We observed c-Ha-ras Tg virgin females to establish the incidence of mammary tumors. A mammary tumor became palpable in 1 of 36 Tg rats at 11 weeks of age, and the tumor incidence gradually increased throughout the observation period, reaching 52.8% (19/36) at 40 weeks (Figure 6). All tumors examined at 35 weeks were adenocarcinomas. In contrast, tumors first became palpable in a non-Tg littermates at 34 weeks and had developed in only 8.4% (2/24) of the 40-week-old animals (Figure 6).

Sporadic alveolar hyperplastic lesions develop in aged Tg rats

Higher populations not only of TEBs but also of ductal epithelial cells were in the proliferative phase in mature virgin Tg rats. At 70 days the number of proliferating cell nuclear antigen-positive nuclei in the ductal epithelium of Tg rats ($n = 3$; Figure 7(D)) was significantly ($P < 0.01$) higher ($15.2 \pm 3.1\%$) than in

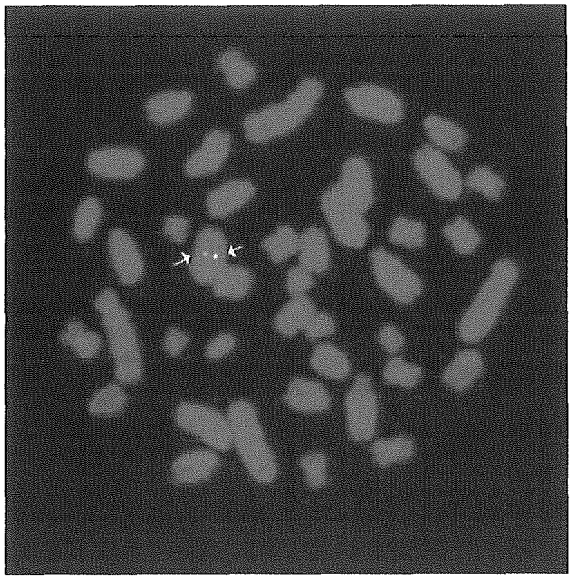

Figure 9. Localization of the human c-Ha-ras transgene in rat chromosomes by fluorescent *in situ* hybridization. The integration site of the transgene was mapped to a single site on chromosome 5, q24–q31.1 (arrows).

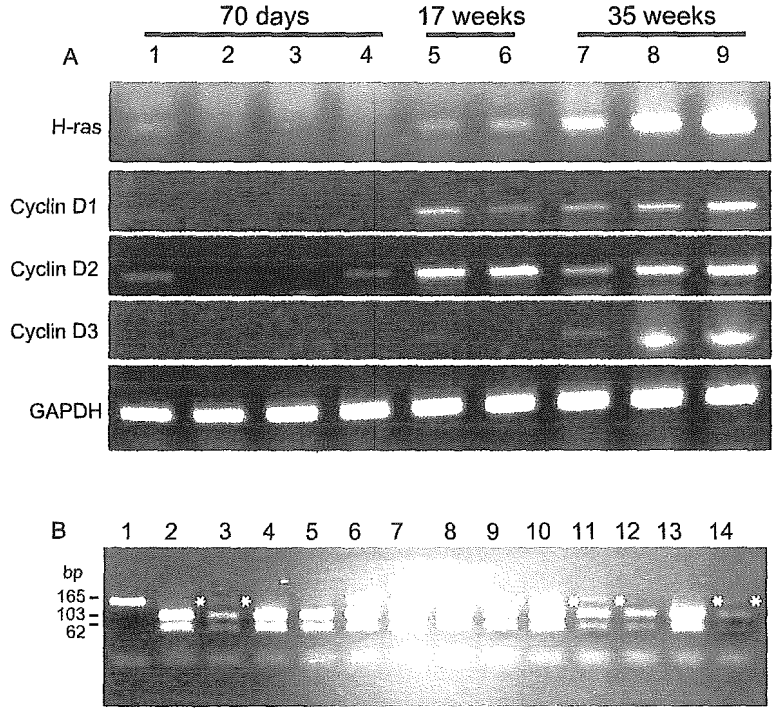

Figure 8. Elevated expression of c-Ha-ras genes in transgenic mammary glands and ras mutations in alveolar hyperplastic nodules. (A) RT-PCR analyses of mRNAs of the human and rat c-Ha-ras (H-ras), and cyclins D1, D2, and D3 in mammary glands from virgin transgenic rats at 70 days and 17 and 35 weeks of age. (B) RFLP analysis of codon 12 of the human c-Ha-ras gene in alveolar hyperplastic nodules. Lane 1, control cDNA of human c-Ha-ras with a mutation; lanes 2, 4, 7, 10, and 13, liver DNAs from five individual transgenic rats; lanes 3, 5, 6, 8, 9, 11, 12, and 14, DNAs from alveolar hyperplastic nodules. Samples were collected from five individual rats (lanes 2 and 3, 4–6, 7–9, 10–12, and 13 and 14). Asterisks indicate faint 165 bp bands corresponding to mutant ras.

that of non-Tg rats ($6.6 \pm 1.1\%$, $n = 3$; Figure 7(C)), although HE-stained samples of Tg mammary glands showed no indication of neoplastic transformation (Figure 7(B)). Examination of 42-week-old mammary glands from non-Tg virgin rats revealed the glands to consist of narrow ducts with a number of alveoli (Figure 7(E) and (H)). By contrast, most of the glands from 35-week-old Tg virgin rats resembled the hormonally stimulated glands normally observed in pregnant animals: there was a marked increase in the number of terminal branches and alveoli, producing diffuse foci of alveolar hyperplasia (Figure 7(F) and (I)). Occasionally the epithelial cells of these pre-neoplastic lesions displayed atypia (Figure 7(G) and (J)).

Alveolar hyperplasia develops in Tg mammary glands with up-regulation of c-Ha-ras protooncogenes and cyclin D family members

We analyzed the expression levels of the human and rat c-Ha-ras genes in 35-week-old Tg mammary glands (Figure 8(A)). From only a few to all of the alveoli in the glands showed hyperplasia with or without cellular atypia (Figure 7). The expression level of the human and rat ras genes was increased at 17 weeks, and there was a more striking increase at 35 weeks, to at least 3.6-fold the level at 70 days. Interestingly, the mRNA levels of cyclins D1 and D2 were increased at 17 weeks and remained high at 35 weeks. Expression of cyclin D3 was also elevated at 35 weeks. The expression profiles of cyclins D1 and D2, but not of cyclin D3, appeared to correlate well with that of the c-Ha-ras genes.

Since alveolar hyperplasia may be pre-neoplastic, we asked the question whether the hyperplastic nodules might contain ras mutations. The human c-Ha-ras transgene was again utilized as a probe. RFLP analysis revealed that six out of eight (75%) of the nodule samples from five rats tested harbored a mutation in codon 12 of the human c-Ha-ras gene, reinforcing the conclusion of a pre-neoplastic nature (Figure 8(B)). However, two samples did not show any mutation

(Figure 8(B), lanes 5, 12), and even in the nodules with ras mutation the cells with the mutation were minor populations, because the two bands (103 and 62 bp) derived from the wild-type ras always predominated over the mutant ras band (165 bp) (Figure 8(B), lanes 3, 6, 8, 9, 11, 14). RFLP analysis detected no mutations of the human c-Ha-ras gene at codon 61 in any of the nodule samples (data not shown), and no mutations at codons 12 and 61 in the liver (Figure 8(B), lanes 2, 4, 7, 10, 13 and data not shown). Based on all of the above findings taken together, we conclude that the hyperplastic change in alveolar hyperplastic nodules is dependent on ras overexpression, not ras mutation.

Chromosome localization of the transgene insertion locus by fluorescent in situ hybridization

Chromosome *in situ* hybridization was carried out on lymphocyte metaphase chromosome spreads with biotin-labeled human c-Ha-ras oligonucleotides as a probe. No chromosomal anomalies such as translocations, duplications, or deletions were observed. Two bright dots were detected on chromosome 5, and the integration site of the transgene was mapped to a single site, q24–q31.1 (Figure 9). Orthologous regions were mapped within mouse chromosome 4, 4.022–4.078 and human chromosome 1p31–1p36.3. No oncogenes or tumor suppressor genes have been mapped in these regions of the rat and the corresponding mouse or human chromosomes. The rat endogenous Ha-ras gene maps to chromosome 1.

Discussion

The present study demonstrated that Tg rats carrying the human c-Ha-ras protooncogene highly susceptible to mammary chemical carcinogens have higher number of TEBs with a higher level of active MAPK compared to non-Tg littermates. A close correlation was noted between the number of TEBs and tumorigenic response initiated by DMBA. Furthermore, a single injection of MNU caused mutations of the c-Ha-ras transgene in TEBs. By contrast, the Tg rats spontaneously developed alveolar hyperplasia with high expression level of c-Ha-ras protooncogene. This can occur without mutations of the transgene.

Human tumors very frequently express ras proteins that have been activated by point mutations-around 20% of all tumors appear to undergo an activating mutation in one of the ras genes [8, 9, 36]. In many instances, such alteration is already present in premalignant lesions, indicating a role in early stages of carcinogenesis [36]. Our c-Ha-ras Tg rats have higher number of TEBs compared to non-Tg littermates (Figure 1), and mutations of the transgene were detected in TEBs before development of carcinomas (Figure 5). This is the first direct evidence demonstrating that ras mutations caused by a chemical carcinogen take place in TEBs. The close correlation observed between the TEB numbers (Figure 1) and the tumor numbers/rat in Tg (Figure 3(D) and Table 2) as well as non-Tg (Figure 3(C) and Table 1) rats provides further support for TEBs being the major targets of chemical carcinogens. We propose that higher TEB numbers at least in part underlie high susceptibility to mammary carcinogenesis of Tg rats.

Not only TEB numbers but also proliferative features of the mammary gland are important for susceptibility. Whereas the TEB number of Tg rats becomes same as that of non-Tg rats by 91 days old of age (Figure 1(B)), the tumor numbers/rat inoculated DMBA at 15 or 20 weeks old of age remains 6–9 times higher in Tg rats than in non-Tg animals at 8 weeks after the treatment (Figure 3(C) and (D)). We have observed higher cell proliferation in the TEBs (Figure 2) and extremely rapid tumor growth in Tg rats [30]. In addition, the mammary glands of Tg rats show elevated expression levels of H-ras, c-myc and cyclin D protooncogenes during sexual maturation (Y. Matsuoka, unpublished data). Therefore, the highly proliferative feature of the mammary gland may be more or at least equally fundamental with TEB numbers regarding the high susceptibility for carcinogenesis in Tg rats. Our results further support the hypothesis proposed by Kumar et al. that normal physiological proliferative processes lead to development of carcinomas if the targeted cells harbor latent ras oncogenes [13].

Ras acts through the MAPK pathway and induces cyclin D1 by acting on the cyclin D1 promoter [37–39]. Cyclin D1 levels are greatly increased in human atypical ductal hyperplasia [40], and the encoding gene is overexpressed in over 50% of human mammary carcinomas [41, 42]. Yu et al. found that expression of ras and neu/erbB-2 oncogenes leads to exclusive induction of cyclin D1 in mouse mammary epithelial cells, whereas expression of c-myc and Wnt-1 results in induction of both cyclins D1 and D2 [23]. Importantly, both cyclin D1 [43] and c-erbB-2 [44] Tg animals develop mammary hyperplasia and carcinomas. Thus, it is very likely that c-Ha-ras pro-

tooncogene induces a type of alveolar hyperplasia as shown in the Tg rats (Figure 7) that is absolutely dependent on cyclin D1. However, we cannot rule out possible involvement of cyclin D2 in formation of the lesions because of its increase in parallel with cyclin D1 (Figure 8(A)), apparently through elevation of the expression of other protooncogenes, such as c-myc and Wnt-1.

Carcinomas are derived via multiple intermediate stages from cells de-differentiating from the normal epithelial lineage. Studying the early stages of mammary neoplasia should provide the foundation for identification of appropriate cellular and molecular targets for therapeutic or preventive intervention. The two general types of lesions with potential to develop into malignancies are alveolar hyperplasia (lobular hyperplasia in humans) and ductal hyperplasia [2, 45, 46]. Recent studies indicate that numerous genes are dysregulated in mouse mammary carcinomas but that few of them, including cell cycle control genes, are altered in alveolar hyperplasia [47]. Transplant experiments using alveolar hyperplastic nodules have demonstrated up-regulation of cyclins B1, D1, and E, and a downregulation of $p21^{WAF1}$ and $p16^{INK4a}$ in the lesions compared to normal mammary tissue [46, 47]. Since levels of cyclins D1 and D2 were here found to be increased in alveolar hyperplasia of our Tg rats (Figure 8(A)), they may serve as an excellent tool for testing the molecules as targets for preventive intervention at the pre-neoplastic stage.

Our Tg rats develop ductal hyperplasia, a type of pre-neoplastic lesion, as well early as 15 days after exposure to a chemical carcinogen [30]. Given the structural and functional resemblance of rat mammary neoplasias to their human counterparts, further elucidation of their biological properties should be of help in conquering the human disease.

Acknowledgements

We are grateful to Drs Y. Matsuda for help with karyotyping of rat lymphocytes, S. Fukushima for suggestions and encouragement and M. Moore for critical reading of the manuscript. We also thank Ms A. Yamaguchi for technical and Ms A. Ichikawa for secretarial assistance. This work was supported in part by a Grant-in-aid for Scientific Research on Priority Areas (KAKENHI) from the Ministry of Education, Science, Sports, and Culture of Japan, a Grant-in-aid for the Second Term Comprehensive 10-Year Strategy for Cancer Control, a Grant-in-aid for Cancer Research, Health and Labor Science Research Grant for Research on Food and Chemical Safety from the Ministry of Health, Labour and Welfare of Japan, and a Grant-in Aid for The Long-range Research Initiative from the Japan Chemical Industry Association (CC05-01). T. Hamaguchi and K. Fukamachi are recipients of research resident fellowships from the Foundation for Promotion of Cancer Research in Japan, supported by the Second Term Comprehensive 10-Year Strategy for Cancer Control.

References

1. Russo J, Wilgus G, Russo IH: Susceptibility of the mammary gland to carcinogenesis: I Differentiation of the mammary gland as determinant of tumor incidence and type of lesion. Am J Pathol 96: 721–736, 1979
2. Russo J, Russo IH: Experimentally induced mammary tumors in rats. Breast Cancer Res Treat 39: 7–20, 1996
3. Sukumar S, McKenzie K, Chen Y: Animal models for breast cancer. Mutat Res 333: 37–44, 1995
4. Thompson HJ, McGinley JN, Rothhammer K, Singh M: Rapid induction of mammary intraductal proliferations, ductal carcinoma *in situ* and carcinomas by the injection of sexually immature female rats with 1-methyl-1-nitrosourea. Carcinogenesis 16: 2407–2411, 1995
5. Thompson HJ, McGinley JN, Wolfe P, Singh M, Steele VE, Kelloff GJ: Temporal sequence of mammary intraductal proliferations, ductal carcinomas *in situ* and adenocarcinomas induced by 1-methyl-1-nitrosourea in rats. Carcinogenesis 19: 2181–2185, 1998
6. Russo J, Russo IH: Biological and molecular bases of mammary carcinogenesis. Lab Invest 57: 112–137, 1987
7. Humphreys RC: Programmed cell death in the terminal endbud. J Mammary Gland Biol Neoplasia 4: 213–220, 1999
8. Schuller HM: Mechanisms of smoking-related lung and pancreatic adenocarcinoma development. Nat Rev Cancer 2: 455–463, 2002
9. Grady WM, Markowitz SD: Genetic and epigenetic alterations in colon cancer. Annu Rev Genomics Hum Genet 3: 101–128, 2002
10. Sukumar S, Notario V, Martin-Zanca D, Barbacid M: Induction of mammary carcinomas in rats by nitroso-methylurea involves malignant activation of H-ras-1 locus by single point mutations. Nature 306: 658–661, 1983
11. Leon J, Kamino H, Steinberg JJ, Pellicer A: H-ras activation in benign and self-regressing skin tumors (keratoacanthomas) in both humans and an animal model system. Mol Cell Biol 8: 786–793, 1988
12. Asamoto M, Ochiya T, Toriyama-Baba H, Ota T, Sekiya T, Terada M, Tsuda H: Transgenic rats carrying human c-Ha-ras proto-oncogenes are highly susceptible to *N*-methyl-

N-nitrosourea mammary carcinogenesis. Carcinogenesis 21: 243–249, 2000
13. Kumar R, Sukumar S, Barbacid M: Activation of ras oncogenes preceding the onset of neoplasia. Science 248: 1101–1114, 1990
14. Filmus J, Robles AI, Shi W, Wong MJ, Colombo LL, Conti CJ: Induction of cyclin D1 overexpression by activated ras. Oncogene 9: 3627–3633, 1994
15. Reuther GW, Der CJ: The Ras branch of small GTPases: ras family members don't fall far from the tree. Curr Opin Cell Biol 12: 157–165, 2000
16. Miyakis S, Sourvinos G, Spandidos DA: Differential expression and mutation of the ras family genes in human breast cancer. Biochem Biophys Res Commun 251: 609–612, 1998
17. Bieche I, Lidereau R: Genetic alterations in breast cancer. Genes Chromosomes Cancer 14: 227–251, 1995
18. Knepper JE, Kittrell FS, Medina D, Butel JS: Spontaneous progression of hyperplastic outgrowths of the D1 lineage to mammary tumors: expression of mouse mammary tumor virus and cellular proto-oncogenes. Mol Carcinog 1: 229–238, 1989
19. Salh B, Marotta A, Matthewson C, Ahluwalia M, Flint J, Owen D, Pelech S: Investigation of the Mek-MAP kinase-Rsk pathway in human breast cancer. Anticancer Res 19: 731–740, 1999
20. von Lintig FC, Dreilinger AD, Varki NM, Wallace AM, Casteel DE, Boss GR: Ras activation in human breast cancer. Breast Cancer Res Treat 62: 51–62, 2000
21. Andres AC, Schonenberger CA, Groner B, Hennighausen L, LeMeur M, Gerlinger P: Ha-ras oncogene expression directed by a milk protein gene promoter: tissue specificity, hormonal regulation, and tumor induction in transgenic mice. Proc Natl Acad Sci USA 84: 1299–1303, 1987
22. Thompson TA, Kim K, Gould MN: Harvey ras results in a higher frequency of mammary carcinomas than Kirsten ras after direct retroviral transfer into the rat mammary gland. Cancer Res 58: 5097–5104, 1998
23. Yu Q, Geng Y, Sicinski P: Specific protection against breast cancers by cyclin D1 ablation. Nature 411: 1017–1021, 2001
24. Kauffmann-Zeh A, Rodriguez-Viciana P, Ulrich E, Gilbert C, Coffer P, Downward J, Evan G: Suppression of c-Myc-induced apoptosis by Ras signalling through PI(3)K and PKB. Nature 385: 544–548, 1997
25. Peli J, Schroter M, Rudaz C, Hahne M, Meyer C, Reichmann E, Tschopp J: Oncogenic Ras inhibits Fas ligand-mediated apoptosis by downregulating the expression of Fas. Embo J 18: 1824–1831, 1999
26. Kazama H, Yonehara S: Oncogenic K-Ras and basic fibroblast growth factor prevent Fas-mediated apoptosis in fibroblasts through activation of mitogen-activated protein kinase. J Cell Biol 148: 557-566, 2000
27. Ries S, Biederer C, Woods D, Shifman O, Shirasawa S, Sasazuki T, McMahon M, Oren M, McCormick F: Opposing effects of Ras on p53: transcriptional activation of mdm2 and induction of p19ARF. Cell 103: 321–330, 2000
28. Ota T, Asamoto M, Toriyama-Baba H, Yamamoto F, Matsuoka Y, Ochiya T, Sekiya T, Terada M, Akaza H, Tsuda H: Transgenic rats carrying copies of the human c-Ha-ras proto-oncogene exhibit enhanced susceptibility to *N*-butyl-*N*-(4-hydroxybutyl)nitrosamine bladder carcinogenesis. Carcinogenesis 21: 1391-1396, 2000
29. Tsuda H, Asamoto M, Ochiya T, Toriyama-Baba H, Naito A, Ota T, Sekiya T, Terada M: High susceptibility of transgenic rats carrying the human c-Ha-ras proto-oncogene to chemically-induced mammary carcinogenesis. Mutat Res 477: 173–182, 2001
30. Matsuoka Y: Rapid emergence of mammary preneoplastic and malignant lesions in human c-Ha-ras proto-oncogene transgenic rats: possible application for screening of chemopreventive agents. Toxicol Pathol (in press)
31. Han BS, Fukamachi K, Takasuka N, Ohnishi T, Maeda M, Yamasaki T, Tsuda H: Inhibitory effects of 17beta-estradiol and 4-*n*-octylphenol on 7,12-dimethylbenz[a]anthracene-induced mammary tumor development in human c-Ha-ras proto-oncogene transgenic rats. Carcinogenesis 23: 1209–1215, 2002
32. Matsuoka Y, Li X, Bennett V: Adducin is an *in vivo* substrate for protein kinase C: phosphorylation in the MARCKS-related domain inhibits activity in promoting spectrin–actin complexes and occurs in many cells, including dendritic spines of neurons. J Cell Biol 142: 485–497, 1998
33. Fukamachi K, Matsuoka Y, Ohno H, Hamaguchi T, Tsuda H: Neuronal leucine-rich repeat protein-3 amplifies MAPK activation by epidermal growth factor through a carboxyl-terminal region containing endocytosis motifs. J Biol Chem 277: 43549–43552, 2002
34. Fukamachi K, Matsuoka Y, Kitanaka C, Kuchino Y, Tsuda H: Rat neuronal leucine-rich repeat protein-3: cloning and regulation of the gene expression. Biochem Biophys Res Commun 287: 257–263, 2001
35. Matsuda Y, Chapman VM: Application of fluorescence *in situ* hybridization in genome analysis of the mouse. Electrophoresis 16: 261–272, 1995
36. Bos JL: Ras oncogenes in human cancer: a review. Cancer Res 49: 4682–4689, 1989
37. Albanese C, Johnson J, Watanabe G, Eklund N, Vu D, Arnold A, Pestell RG: Transforming p21ras mutants and c-Ets-2 activate the cyclin D1 promoter through distinguishable regions. J Biol Chem 270: 23589–23597, 1995
38. Liu JJ, Chao JR, Jiang MC, Ng SY, Yen JJ, Yang-Yen HF: Ras transformation results in an elevated level of cyclin D1 and acceleration of G1 progression in NIH 3T3 cells. Mol Cell Biol 15: 3654–3663, 1995
39. Lavoie JN, L'Allemain G, Brunet A, Muller R, Pouyssegur J: Cyclin D1 expression is regulated positively by the p42/p44MAPK and negatively by the p38/HOGMAPK pathway. J Biol Chem 271: 20608–20616, 1996
40. Steeg PS, Zhou Q: Cyclins and breast cancer. Breast Cancer Res Treat 52: 17–28, 1998
41. Bartkova J, Lukas J, Muller H, Lutzhoft D, Strauss M, Bartek J: Cyclin D1 protein expression and function in human breast cancer. Int J Cancer 57: 353–361, 1994
42. Gillett C, Fantl V, Smith R, Fisher C, Bartek J, Dickson C, Barnes D, Peters G: Amplification and overexpression of cyclin D1 in breast cancer detected by immunohistochemical staining. Cancer Res 54: 1812–1817, 1994
43. Wang TC, Cardiff RD, Zukerberg L, Lees E, Arnold A, Schmidt EV: Mammary hyperplasia and carcinoma in MMTV-cyclin D1 transgenic mice. Nature 369: 669–671, 1994

44. Davies BR, Platt-Higgins AM, Schmidt G, Rudland PS: Development of hyperplasias, preneoplasias, and mammary tumors in MMTV-c-erbB-2 and MMTV-TGFalpha transgenic rats. Am J Pathol 155: 303–314, 1999
45. Singh M, McGinley JN, Thompson HJ: A comparison of the histopathology of premalignant and malignant mammary gland lesions induced in sexually immature rats with those occurring in the human. Lab Invest 80: 221–231, 2000
46. Medina D: Biological and molecular characteristics of the premalignant mouse mammary gland. Biochim Biophys Acta 1603: 1–9, 2002
47. Said TK, Medina D: Cell cyclins and cyclin-dependent kinase activities in mouse mammary tumor development. Carcinogenesis 16: 823–830, 1995

Address for offprints and correspondence: Dr Yoichiro Matsuoka, Experimental Pathology and Chemotherapy Division, National Cancer Center Research Institute, 5-1-1 Tsukiji, Chuo-ku, Tokyo 104-0045, Japan; *Tel.:* +81-3-3542-2511; *Fax:* +81-3-3542-3586; *E-mail:* yomatsuo@gan2.res.ncc.go.jp, or Dr Hiroyuki Tsuda Department of Molecular Toxicology, Nagoya City University Graduate School of Medical Sciences, 1 Kawasumi, Mizuho-cho, Mizuho-ku, Nagoya 467-8601, Japan; *Tel.:* +81-52-853-8991; *Fax:* +81-52-853-8996; *E-mail:* htsuda@med.nagoya-cu.ac.jp

[CANCER RESEARCH 64, 1794–1801, March 1, 2004]

Inhibition of Metastasis of Tumor Cells Overexpressing Thymidine Phosphorylase by 2-Deoxy-L-Ribose

Yuichi Nakajima,[1] Takenari Gotanda,[1] Hiroshi Uchimiya,[1] Tatsuhiko Furukawa,[1] Misako Haraguchi,[1] Ryuji Ikeda,[1] Tomoyuki Sumizawa,[1] Hiroki Yoshida,[2] and Shin-ichi Akiyama[1]

Departments of [1]Molecular Oncology and [2] Tumor Pathology, Field of Oncology, Course of Advanced Therapeutics, Graduate School of Medical and Dental Science, Kagoshima University, Kagoshima Japan

ABSTRACT

Thymidine phosphorylase (TP) catalyzes the reversible conversion of thymidine to thymine, thereby generating 2-deoxy-D-ribose-1-phosphate, which upon dephosphorylation forms 2-deoxy-D-ribose (D-dRib), a degradation product of thymidine. We have previously shown that D-dRib promotes angiogenesis and chemotaxis of endothelial cells and also confers resistance to hypoxia-induced apoptosis in some cancer cell lines. 2-Deoxy-L-ribose (L-dRib), a stereoisomer of D-dRib, can inhibit D-dRib anti-apoptotic effects and suppressed the growth of KB cells overexpressing TP (KB/TP cells) transplanted into nude mice. In this study, we examined the ability of L-dRib to suppress metastasis of KB/TP cells using two different models of metastasis. The antimetastatic effect of L-dRib was first investigated in a liver-metastasis model in nude mice inoculated with KB/TP cells. Oral administration of L-dRib for 28 days at a dose of 20 mg/kg/day significantly reduced the number of metastatic nodules in the liver and suppressed angiogenesis and enhanced apoptosis in KB/TP metastatic nodules. Next, we compared the ability of L-dRib and tegafur alone or in combination to decrease the number of metastatic nodules in organs in the abdominal cavity in nude mice receiving s.c. of KB/TP cells into their backs. L-dRib (20 mg/kg/day) was significantly ($P < 0.05$) more efficient than tegafur (100 mg/kg/day) in decreasing the number of metastatic nodules in organs in the abdominal cavity. By *in vitro* invasion assay, L-dRib also reduced the number of invading KB/TP cells. L-dRib anti-invasive activity may be mediated by its ability to suppress the enhancing effect of TP and D-dRib on both mRNA and protein expression of vascular endothelial growth factor and interleukin-8 in cultured KB cells. These findings suggest that L-dRib may be useful in a clinical setting for the suppression of metastasis of tumor cells expressing TP.

INTRODUCTION

Tumor metastasis is a complex process. Neo-vascularization is essential for both primary and metastatic tumor growth (1, 2). Various angiogenic factors that are produced by solid tumors have been identified (3–6). Angiogenesis is regulated by a balance between pro-angiogenic factors and inhibitors of angiogenesis (7). Manipulation of these factors for anti-angiogenic therapy is a new and promising avenue in cancer treatment. Anti-angiogenic therapy may be effective for a broad spectrum of tumors, may have fewer side effects, and may be less inductive to the emergence of drug resistant tumor cells (8).

We previously reported that thymidine phosphorylase (TP) is identical to platelet-derived endothelial cell growth factor and is a potent angiogenic factor that plays a key role in tumor angiogenesis (9–11). Many types of solid tumors express TP and high TP activity is correlated with microvessel density (12–15). In addition to angiogenic activity, TP can suppress hypoxia-induced apoptosis (16). TP catalyzes the reversible phosphorolysis of thymidine and other pyrimidine 2′-deoxyribonucleosides. The conversion of thymidine to thymine and 2-deoxy-D-ribose-1-phosphate by TP activity generates a dephosphorylated product 2-deoxy-D-ribose (D-dRib). D-dRib mediates many of the biological activities of TP. Thus D-dRib displays angiogenic activity in the chorioallantoic membrane assay (17). D-dRib has also been shown to stimulate chemotaxis and tubular formation of endothelial cells and enhanced the growth of tumors by conferring resistance to hypoxia-induced apoptosis on the tumor cells (11, 18, 19). Inhibition of the functions of TP and D-dRib may, therefore, prove to be useful in the inhibition of tumor growth and metastasis of TP-expressing tumor cells.

Several novel inhibitors of TP have recently been reported (20). One of these, TP inhibitor, could suppress the effect of TP-mediated angiogenesis, tumor growth, metastasis, and resistance to hypoxia-induced apoptosis (11). However the use of these inhibitors as anti-tumor agents has a number of drawbacks because they directly inhibit TP activity. Firstly, the inhibition of TP activity could lead to increased thymidine levels in plasma that may be toxic. Nishino *et al.* have reported that patients with mitochondrial neurogastrointestinal encephalomyopathy who had very low TP activity in their plasma because of homozygous mutations in their TP genes showed pathological changes in the brain and muscle because of mitochondrial alterations (21, 22). Secondly, TP activity is required for the activation of the cytotoxic activities of other antitumor drugs such as 5′-dFUrd and tegafur (23). We have demonstrated that TP-transfected human carcinoma KB cells overexpressing TP (KB/TP cells) are more sensitive to these drugs than parental cells (24). Therefore, it will be difficult to use TP inhibitor in combination with 5′-dFUrd and its prodrugs. For these reasons, inhibition of D-dRib, the downstream mediator of TP functions, would be a more preferable target for antitumor therapy than direct inhibition of TP activity.

We have previously reported that the various effects of D-dRib could be inhibited by 2-deoxy-L-ribose (L-dRib), a stereoisomer of D-dRib. L-dRib has been shown to inhibit chemotaxis and tubulogenesis of bovine aortic endothelial cells induced by D-dRib (18), to suppress angiogenesis induced by KB/TP cells in a dorsal air sac assay, and to suppress the growth of KB/TP cells that are xenografted into nude mice. L-dRib also increases the proportion of apoptotic cells in the TP-expressing tumors (18). These results demonstrate that L-dRib could be a new type of anticancer drug that inhibits angiogenesis and induces apoptosis of tumor cells expressing TP.

Although direct inhibition of TP activity by TP inhibitor has been shown to prevent liver metastasis of tumor cells expressing TP (25), the ability of L-dRib to inhibit metastasis has not yet been explored. In this study, we, therefore, investigated the ability of L-dRib to suppress metastasis of TP-expressing tumor cells. We further investigated the ability of L-dRib to modulate the invasive activity and the production of angiogenic factors of KB/TP cells *in vitro*.

MATERIALS AND METHODS

Compounds and Reagents. Tegafur was a gift from Taiho pharmaceutical Co., Ltd. (Tokyo, Japan). L-dRib was purchased from Sigma Chemical Co. (St. Louis, MO).

Received 8/20/03; revised 12/11/03; accepted 12/29/03.

The costs of publication of this article were defrayed in part by the payment of page charges. This article must therefore be hereby marked *advertisement* in accordance with 18 U.S.C. Section 1734 solely to indicate this fact.

Requests for reprints: Shin-ichi Akiyama, Department of Molecular Oncology, Field of Oncology, Course of Advanced Therapeutics, Graduate School of Medical and Dental Science, Kagoshima University, Kagoshima Sakuragaoka 8-35-1, Kagoshima 890-8520, Japan. Phone: 81-99-275-5490, Fax: 81-99-265-9687.

Animals and Cell Culture. Six-week old male BALB/c nude mice (CLEA Japan, Inc., Tokyo, Japan) were used. The KB-3-1 cell line, derived from human epidermoid carcinoma cells, was maintained in MEM containing 10% newborn calf serum, 100 units/ml penicillin, and 2 mM L-glutamine.

Transfection of *TP/PD-ECGF* cDNA into KB-3-1 Cells. The *TP/PD-ECGF* full-length cDNA expression vector or the empty vector was transfected into KB-3-1 cells by electroporation (26). After selection with geneticin, the expression of TP in each clone was determined by immunoblot analysis using an anti-TP monoclonal antibody as described previously (27). A TP-positive clone (KB/TP cells) and a control vector-transfected clone (KB/CV cells) were further analyzed.

Experimental Liver Metastasis Model. KB/TP and KB/CV cells were harvested by brief trypsinization, washed twice with PBS, and then suspended in PBS at 10^6 cells/ml. KB/TP or KB/CV cells (10^5 cells) in 0.1 ml PBS were injected into the spleen which was exposed after transverse incision in the left flank of the anesthetized mice (six mice per group). After 1 min, the spleen was removed, and the abdominal incision was closed (25). Liver metastatic nodules were difficult to observe in this metastatic model unless the spleens were extirpated (data not shown). From one day after inoculation, mice were given p.o. L-dRib at a dose of 20 or 100 mg/kg/day every day. The same volume of physiological saline was given to the control mice. Four weeks after tumor inoculation, the number of metastatic nodules on the liver surface was counted under a stereoscopic microscope (25). The extent of the metastatic areas was evaluated from hematoxylin- and eosin-stained liver tissue sections from the left lateral liver lobe. Histological views were captured digitally. The ratio of the area of liver with metastasis to total liver area was calculated using NIH Image (US National Institute of Health) software (28, 29).

Immunohistochemical Staining of Blood Vessels in Metastatic Nodules. The liver tissues were embedded in OCT compound (Sakura Finetek, Torrance, CA), and then frozen quickly in liquid nitrogen and stored at −80°C. Cryosections were fixed in acetone for 2 min at −20°C and then incubated with 0.3% H_2O_2 in PBS for 10 min at room temperature to block endogenous peroxidase activity. After rinsing with PBS, the cryosections were stained for endothelial cells with a rat monoclonal antimouse CD31 antibody (PharMingen, San Diego, CA). Antibody binding was detected by sequential incubation with a biotin-conjugated goat antirat immunoglobulin and a streptavidin-horseradish peroxidase complex (Vector Laboratories Inc., Burlingame, CA). Color development was performed with diaminobenzidine using a substrate kit (Vector Laboratories Inc.). The cryosections were then counterstained with 0.5% methyl green. Three random microscopic fields at ×400 magnification were captured for each metastasis. Histological views were captured digitally. The ratio of the vessel area to the tumor area was calculated using NIH Image software (28, 29).

TUNEL Assay and Evaluation of Apoptosis in Metastatic Nodules. Liver tissues were embedded in paraffin, and then sections were cut into 3 μm. Terminal deoxynucleotidyl transferase-mediated deoxyuridine triphosphate fluorescence nick end labeling (TUNEL) assay was performed using a commercial kit (Intergen Company, Purchase, NY). The TUNEL-positive apoptotic cells were counted in microscopic fields at ×200 magnification. For all sections, apoptotic cells were counted in total areas of the metastatic nodules except the necrotic area. The apoptotic index was calculated as follows: apoptotic index (%) = TUNEL-positive cell number/total cell number ×100. The evaluation was performed twice as a blind study.

Subcutaneous Tumor Model. KB/TP and KB/CV cells were suspended in PBS at 10^7 cells/ml, and 10^6 tumor cells were injected s.c. into the backs of nude mice (six mice per group; eight groups). Consistent with our other data, 100% tumorigenicity was achieved about 1 week after s.c. injection. Drug treatments were initiated from day 3 after tumor inoculation. L-dRib (20 mg/kg/day), tegafur (100 mg/kg/day), L-dRib and tegafur (20 and 100 mg/kg/day), or saline were administered p.o. every day. Mice were sacrificed on day 52, and the number of metastatic nodules on the surface of the intestines was counted (from the duodenum to the rectum).

Invasion Assay. KB/TP and KB/CV cells were cultured in 100-mm dishes to subconfluence. The growth medium was replaced with serum-free medium containing 0.01% BSA (Sigma, Poole, United Kingdom) and 3.3 mM glucose. These cells were routinely maintained at 37°C in a humidified atmosphere of 5% CO_2 and 1% O_2 (hypoxia group) for an additional 24 h. Control cells were placed in a standard incubator under 95% air and 5% CO_2 (normoxia group). For the invasion assay, the BD Bio Coat Matrigel Invasion Chamber (BD Biosciences, Franklin Lakes, NJ), in which the upper and bottom chambers were separated by a Matrigel-coated membrane (8 μm pore), were used according to the protocol of the manufacturer, with some modifications. Briefly, the lower surface of the filters were precoated with collagen (1 μg) in a volume of 60 μl cold PBS and dried overnight at room temperature. The coated filters were washed with serum-free MEM medium before use. KB/TP or KB/CV cells were harvested with 0.02% trypsin containing 0.02% EDTA. Cells (5×10^4) were seeded in each of the upper chambers (24-well chambers) in 0.5 ml of serum-free medium containing 0.01% BSA and 3.3 mM glucose, and the bottom chambers contained the appropriate medium with 1% FBS as a chemoattractant. The KB/TP cells were then treated for 24 h in the absence or presence of L-dRib (10 or 100 μM). The noninvading cells on the upper surface of the filters were removed by wiping with a cotton swab. Cells at the bottom side of the membranes were fixed with ethanol, and stained with 0.5% methyl blue. The number of cells invading through the Matrigel membrane was counted in microscopic fields at ×200 magnification. To minimize bias, at least 3 randomly selected fields were counted. Data were averages of triplicate determinants for each condition.

Real-time Reverse-Transcription PCR Quantification. KB/TP and KB/CV cells were cultured under the conditions described for the invasion assay. KB/TP cells were then treated for 48 h in the absence or presence of L-dRib (10 or 100 μM) or D-dRib (100 μM). KB/CV cells were treated for 48 h in the absence or presence of D-dRib (100 μM). Total RNA from the cultured cells was isolated using TRIzol reagent (Invitrogen, Carlsbad, CA). One

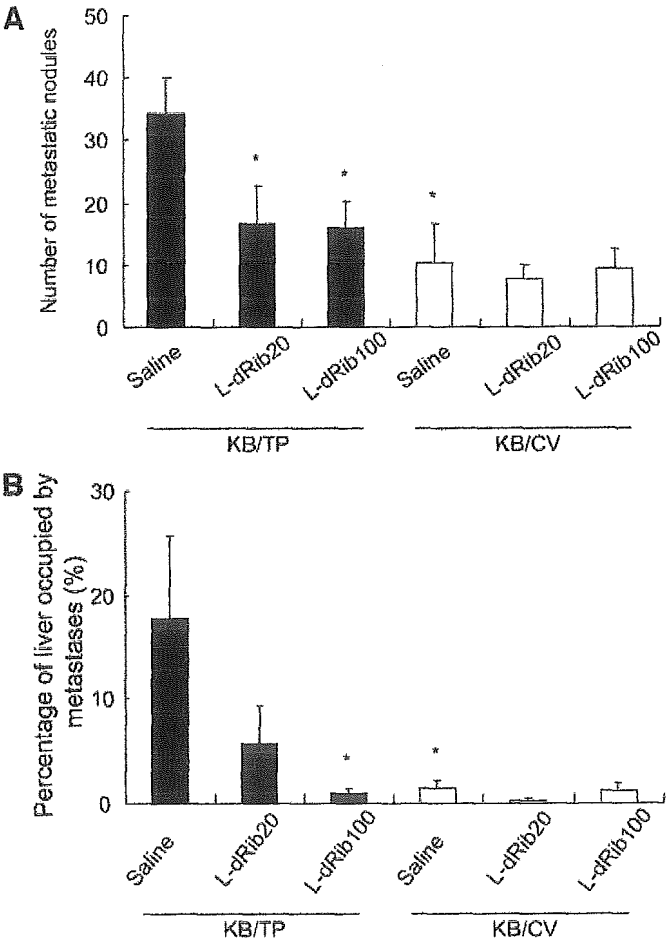

Fig. 1. The effect of 2-deoxy-L-ribose (L-dRib) on thymidine phosphorylase (TP)-mediated tumor metastases. Nude mice were intra intrasplenically inoculated with KB cells over-expressing TP (KB/TP) or the empty vector transfected cells (KB/CV) as a control. From the second day after inoculation, mice were given p.o. L-dRib [20 mg/kg/day (*L-dRib20*) or 100 mg/kg/day (*L-dRib100*)] or control saline every day as indicated. The effect of L-dRib on the numbers of metastatic nodules on the liver surface (*A*) and the percentage of the liver area with metastasis was assayed (*B*). Each *column* and *bar* represents the mean ± SE from six mice per group. *, $P < 0.05$ *versus* KB/TP saline control.

microgram of RNA was reverse transcribed using a first-strand cDNA synthesis kit (ReverTra Ace α, TOYOBO, Osaka, Japan). Human angiogenic factor (*VEGF* and *IL-8*) gene expression levels were assayed by real-time reverse PCR (PRISM 7900HT, Applied Biosystems, Foster City, CA) according to the technical brochure of the company. The sets of primers and TaqMan probes were designed with a primer design software Primer Express version 1.5 (Applied Biosystems). Human *GAPDH* was used for normalization. Quantification of target gene expression was obtained with the comparative cycle threshold method according to the instructions of the manufacturer.

Measurement of Interleukin 8 (IL-8) and Vascular Endothelial Growth Factor (VEGF) in Conditioned Media. KB/TP and KB/CV cells were plated in 35 mm wells at 1×10^5 cells/well and cultured overnight. The growth medium was replaced with serum-free medium containing 0.01% BSA (Sigma) and 3.3 mM glucose. These cells were routinely maintained at 37°C in a humidified atmosphere of 5% CO_2 and 1% O_2 for an additional 48 h. KB/TP cells were then treated for 48 h in the absence or presence of L-dRib (10 or 100 μM). For some experiments KB/CV cells were treated for 48 h in the absence or presence of D-dRib (100 μM).

IL-8 and VEGF levels in the conditioned media were quantified by using an Immunoassay Kit, (BioSource International, Camarillo, CA) according to the manufacturer's instructions. The number of cells in each well was counted with the Sysmex MICROCELL Counter F-300 (Toa, Kobe, Japan).

RESULTS

Effect of L-dRib on Liver Metastasis. The effect of L-dRib on liver metastasis of KB/TP cells was assayed in mice inoculated with KB/TP or control KB/CV cells into the spleen. Treatment with p.o. administered L-dRib at 20 or 100 mg/kg/day was started one day after inoculation of the cells and after 4 weeks the effect of L-dRib on metastasis was measured. Calculation of the mean number of KB/TP metastatic nodules in the liver indicated that administration of L-dRib at 20 and 100 mg/kg/day significantly decreased the number of metastatic nodules from 34 ± 6 (mean ± SE) to 17 ± 6 and 16 ± 4, respectively. The effect of L-dRib on KB/CV metastases was not

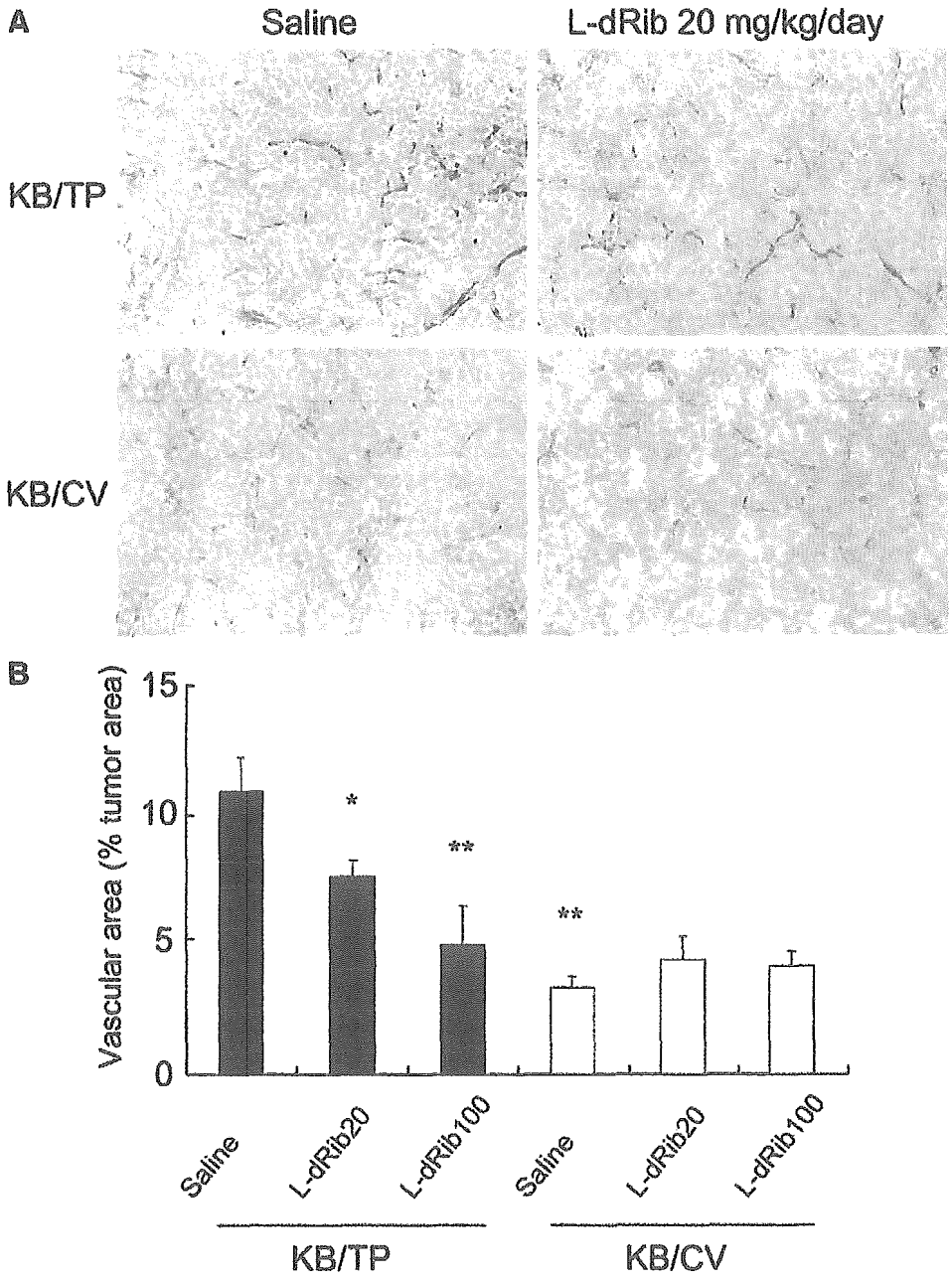

Fig. 2. The effect of L-dRib on TP-mediated tumor angiogenesis in metastatic nodules. *A*, endothelial cells within metastatic nodules of KB/TP or KB/CV in the liver were specifically stained with antimouse CD31 antibody and photographed (×200 magnification). The effect of L-dRib (20 mg/kg/day) or control saline administration on endothelial cells is indicated. *B*, the effect of L-dRib [20 mg/kg/day (*L-dRib20*) or 100 mg/kg/day (*L-dRib100*)] or control saline administration on the mean vessel area, calculated as a percentage of the tumor area is shown. Each *column* and *bar* represents the mean ± SE from six mice per group. *, $P < 0.05$ *versus* KB/TP saline control. **, $P < 0.01$ *versus* KB/TP saline control.

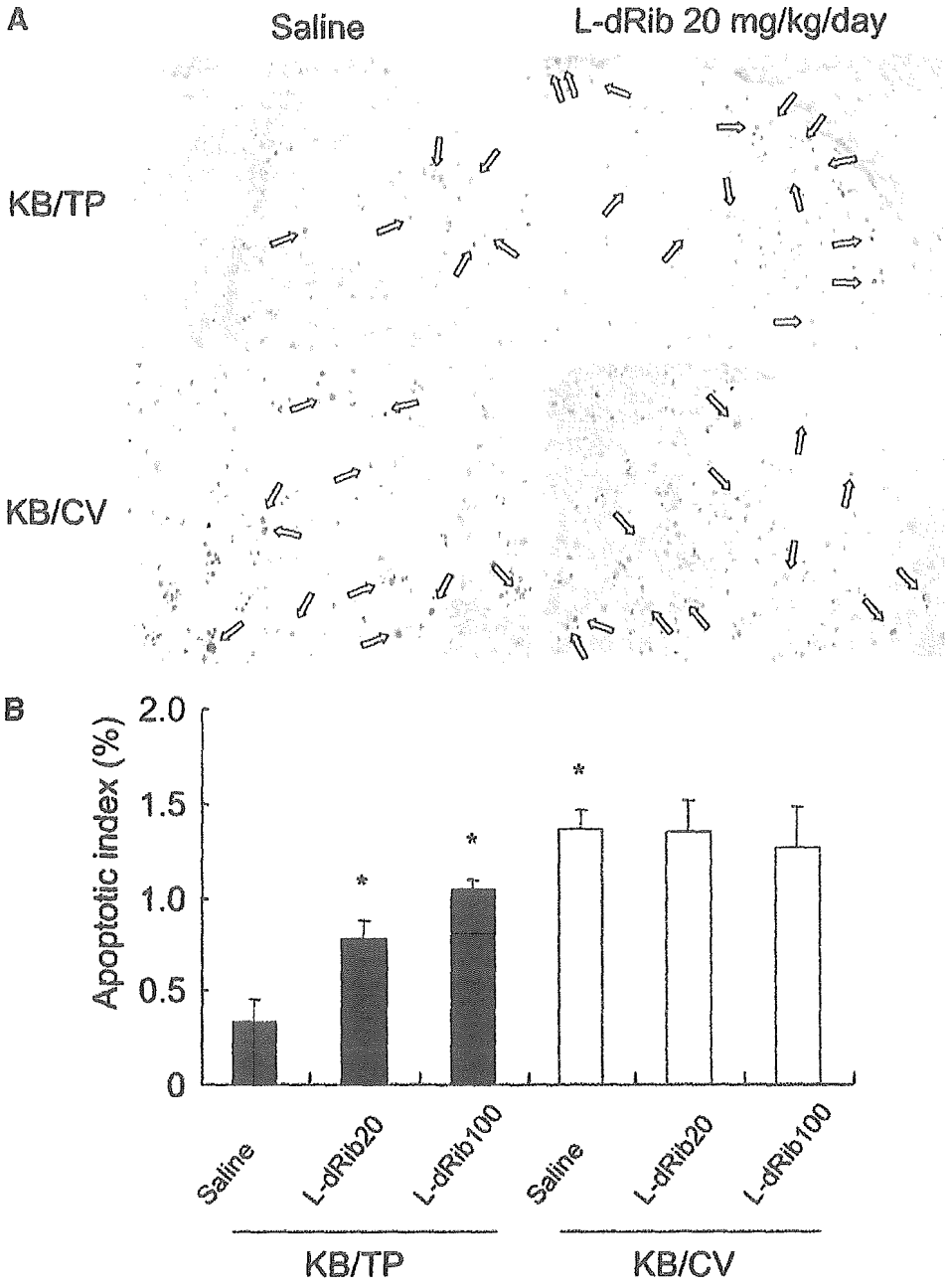

Fig. 3. The effect of L-dRib on apoptosis in metastatic nodules of murine livers. *A*, apoptotic cells in paraffin-embedded fixed sections of metastatic nodules in murine livers of mice inoculated with *KB/TP* or *KB/CV* were detected by the terminal deoxynucleotidyl transferase-mediated deoxyuridine triphosphate fluorescence nick end labeling (TUNEL) assay (×200 magnification) and are indicated by *arrows*. The effect of L-dRib (20 mg/kg/day) or control saline administration is shown. *B*, the apoptotic index, calculated as the percentage of TUNEL-positive cells, is shown for each of the indicated treatments. Each *column* and *bar* represents the mean ± SE from six mice per group. *, $P < 0.05$ *versus* KB/TP saline control.

significant (Fig. 1*A*). Treatment with L-dRib at 20 or 100 mg/kg/day also significantly decreased the mean percentage of the liver area occupied by the KB/TP metastatic nodules from 17.9 ± 7.7% to 5.9 ± 3.5% and 0.9 ± 0.6%, respectively (Fig. 1*B*). These data indicate that L-dRib treatment can significantly decrease both the number of metastatic nodules and the intrahepatic growth of the KB/TP tumors.

Effect of L-dRib on TP-mediated Angiogenesis. The effect of L-dRib on blood vessel formation in liver metastatic nodules from KB/TP or KB/CV tumors was examined by immunohistochemical staining of endothelial cells as shown in Fig. 2*A*. Examination of the tissue sections at low magnification indicated that KB/CV nodules showed more extended necrotic and avascular areas than KB/TP nodules and that L-dRib at 20 mg/kg/day inhibited blood vessel formation in the KB/TP nodules.

The effect of L-dRib on angiogenesis was quantified by determination of the average vessel area as a percentage of the total tumor area. L-dRib treatment at 20 and 100 mg/kg/day reduced the mean vessel area in KB/TP metastatic nodules in the liver by 70.3% ($P < 0.05$) and 45.0% ($P < 0.01$), respectively, compared with untreated mice. L-dRib did not reduce the vessel area in KB/CV nodules (Fig. 2*B*). Thus L-dRib significantly inhibited TP-mediated angiogenesis in a dose-dependent manner.

Effect of L-dRib on TP-Mediated Resistance to Apoptosis. The effect of L-dRib on TP-mediated resistance to apoptosis was determined by measurement of apoptotic cells in metastatic nodules in the liver sections of KB/TP or KB/CV mice treated with either L-dRib or control saline. Apoptotic cells were stained with the TUNEL technique as shown in Fig. 3*A* and quantified as a percentage of the total cells in the metastatic nodules as shown in Fig. 3*B*.

The apoptotic index in KB/TP metastatic nodules was 4-fold lower than in KB/CV metastatic nodules. Treatment with L-dRib at 20 and

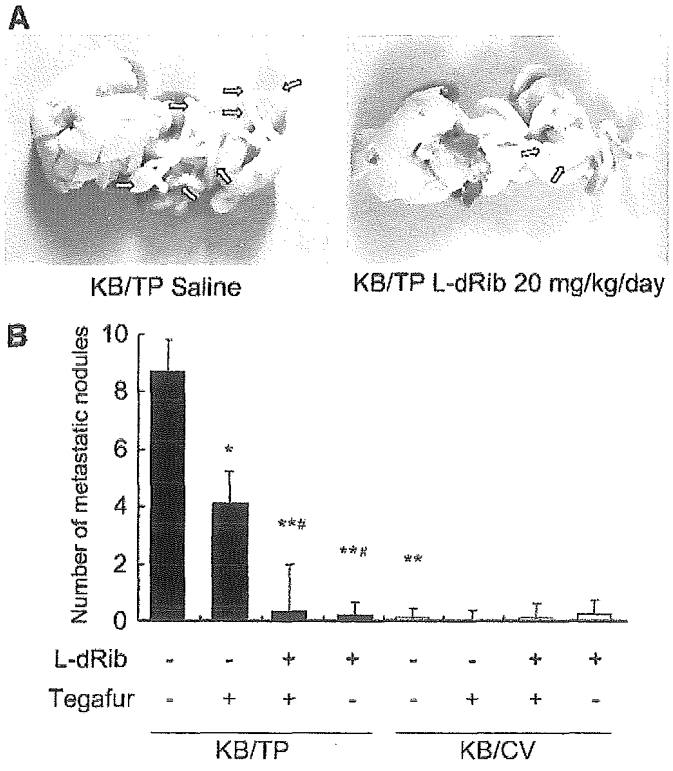

Fig. 4. Inhibition of TP-mediated tumor growth and metastases by L-dRib. *KB/TP* or the empty vector transfected cells (*KB/CV*) were injected into the shoulders of nude mice. From the fourth day after inoculation, mice were treated with either saline, L-dRib (20 mg/kg/day), tegafur (100 mg/kg/day), or L-dRib and tegafur (20 and 100 mg/kg/day), respectively every day. *A*, photographs of the metastatic nodules on the surface of intestines from KB/TP tumors treated with saline alone (*left*) or 20 mg/kg/day L-dRib (*right*). *Arrows* indicate metastatic nodules. *B*, the number of metastatic nodules on the intestinal surface from duodenum to rectum was counted using a stereoscopic microscope after the indicated treatments with L-dRib and/or tegafur. All results are the mean ± SE from six mice per group. *, $P < 0.05$ and **, $P < 0.01$ *versus* KB/TP saline control. #, $P < 0.05$ *versus* KB/TP tumors treated with tegafur alone.

100 mg/kg/day increased the proportion of apoptotic tumor cells 2.3- and 3.1-fold respectively in KB/TP nodules compared with untreated nodules. However no difference in the proportion of apoptotic tumor cells was found between treated and untreated KB/CV nodules (Fig. 3).

Combination Chemotherapy of Tumors with L-dRib and Tegafur. The above data suggested that L-dRib might be an effective antitumor agent preferentially acting on tumors that overexpress TP. We therefore determined the ability of L-dRib to modulate blood-borne metastasis either alone, or in combination with tegafur. Tegafur is an antitumor agent that requires TP activity for its activation. Because L-dRib inhibits TP-induced downstream functions but not its enzymatic activity, tegafur should be activated in the presence of L-dRib and the combination therapy of L-dRib and tegafur should be effective against TP-expressing tumors. As a control the effect of tegafur alone was also monitored.

Concerning the s.c. tumor model, all mice survived to day 52. We first compared the ability of L-dRib and tegafur to reduce the number of KB/TP metastatic nodules in the intestine of nude mice s.c. injected with KB/TP cells into their backs. Oral administration of L-dRib (20 mg/kg/day) inhibited the formation of metastatic nodules as shown in the photograph in Fig. 4*A*. Furthermore L-dRib was more efficient in reducing the number of KB/TP nodules than tegafur (100 mg/kg/day) as quantified in Fig. 4*B*. Neither L-dRib nor tegafur had any significant effects on body weight or general condition of the mice (data not shown). Also, neither L-dRib nor tegafur reduced the metastatic nodules in KB/CV mice in which the number of metastatic nodules was significantly lower than in KB/TP mice. When L-dRib and tegafur were tested in combination the effect on the number of KB/TP metastatic nodules was similar to that of L-dRib alone (Fig. 4*B*). Thus L-dRib is more effective than tegafur in the suppression of TP-mediated metastasis of KB/TP cells. The number and size of the metastatic nodules of KB/TP cells were augmented compared with those of KB/CV cells. The metastatic nodules of KB/TP cells, but not of KB/CV cells, invaded in subserosal muscularis, and L-dRib attenuated the invasion. The mean size of KB/TP tumors (3220.0 ± 389.3 mm^3) was 1.29-fold larger than that of KB/CV tumors (2494.6 ± 385.0 mm^3). The sizes of the KB/TP tumors in mice treated with L-dRib (20 mg/kg/day), tegafur (100 mg/kg/day), or L-dRib and tegafur (20 and 100 mg/kg/day), were 24, 64 or 71% of that in control mice. We could not detect macroscopic and microscopic metastasis at other organs besides intestine. The very effective reduction of metastatic nodules by L-dRib and less effective reduction of the nodules by tegafur suggests that combination chemotherapy of L-dRib and tegafur would be needed to suppress both tumor growth and metastasis.

Effect of L-dRib on TP-mediated Tumor-cell Invasion. To examine the mechanism by which L-dRib modulates KB/TP metastasis, we investigated the effect of L-dRib on invasion of KB/TP cells *in vitro* in Matrigel invasion assays. Because the invasive activity of KB/TP cells is higher than of KB/CV cells under hypoxic conditions the assay was carried out under hypoxic as well as normoxic conditions (Fig. 5). The addition of L-dRib (100 μM) to the medium significantly reduced the number of invading KB/TP cells under hypoxic conditions. In contrast L-dRib did not significantly reduce the number of invading KB/CV cells (data not shown) although the invasive activity of KB/CV cells was stimulated by D-dRib. Thus L-dRib selectively inhibits the invasion of KB/TP cells.

Effect of L-dRib on the TP-Mediated Expression of *VEGF* and *IL-8* Genes. We next examined whether L-dRib might inhibit the invasion of KB/TP cells by suppressing the expression of the pro-invasive factors VEGF and IL-8 that are induced by TP and its downstream effector D-dRib in cultured KB cells. D-dRib increased

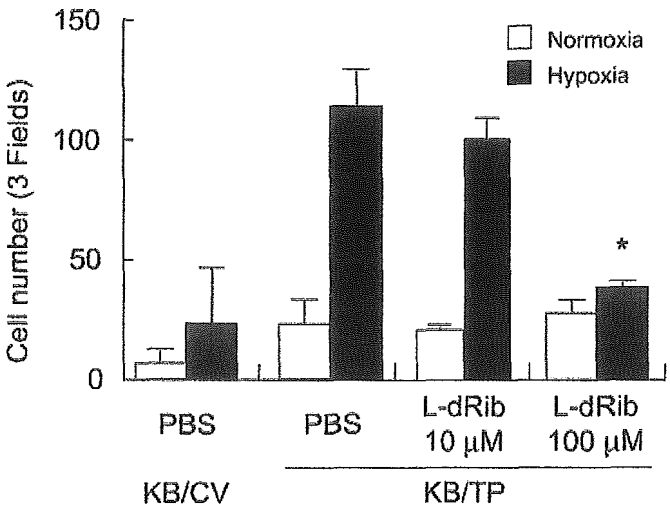

Fig. 5. Effect of L-dRib on cell invasiveness in the Matrigel basement membrane cell-invasion chamber. KB/TP or KB/CV that were cultured in serum starved medium under normoxic (*open columns*) or hypoxic conditions (*closed columns*) for 24 h were seeded on Matrigel-coated filters. Invasion was allowed to proceed for 24 h in the presence or absence of 10 μM or 100 μM L-dRib or with PBS as indicated. Cells in three randomly selected fields were counted for each treatment. The data are averages of triplicate determinants. Each *bar* represents the mean ± SD. *, $P < 0.05$ *versus* KB/TP cells treated with PBS.

the expression levels of these genes in KB/CV cells only under hypoxic conditions (Fig. 6). The expression levels of *VEGF* and *IL-8* mRNAs were up-regulated in KB/TP cells under hypoxic conditions compared with KB/CV cells. In particular, the expression level of *IL-8* mRNA in KB/TP cells was more than that 18-fold higher than that in KB/CV cells (Fig. 6*B*). L-dRib significantly decreased the expression of both *VEGF* (50% decrease) and *IL-8* mRNA (80% decrease) in KB/TP cells under hypoxic conditions.

Effect of L-dRib on TP-Mediated Secretion of VEGF and IL-8. Because mRNA levels do not always correlate with protein levels, we further examined whether *VEGF* and *IL-8* mRNA levels correlate with the levels of these proteins secreted from KB cells. We, thus, measured VEGF and IL-8 protein levels in conditioned media from KB/TP or KB/CV cells using an ELISA assay. Although the mRNA and protein levels do not exactly correlate, the secreted protein levels of VEGF and IL-8 from KB/TP cells were higher than those from KB/CV cells (Fig. 7). Thus, TP appears to augment VEGF and IL-8 production and release from KB cells.

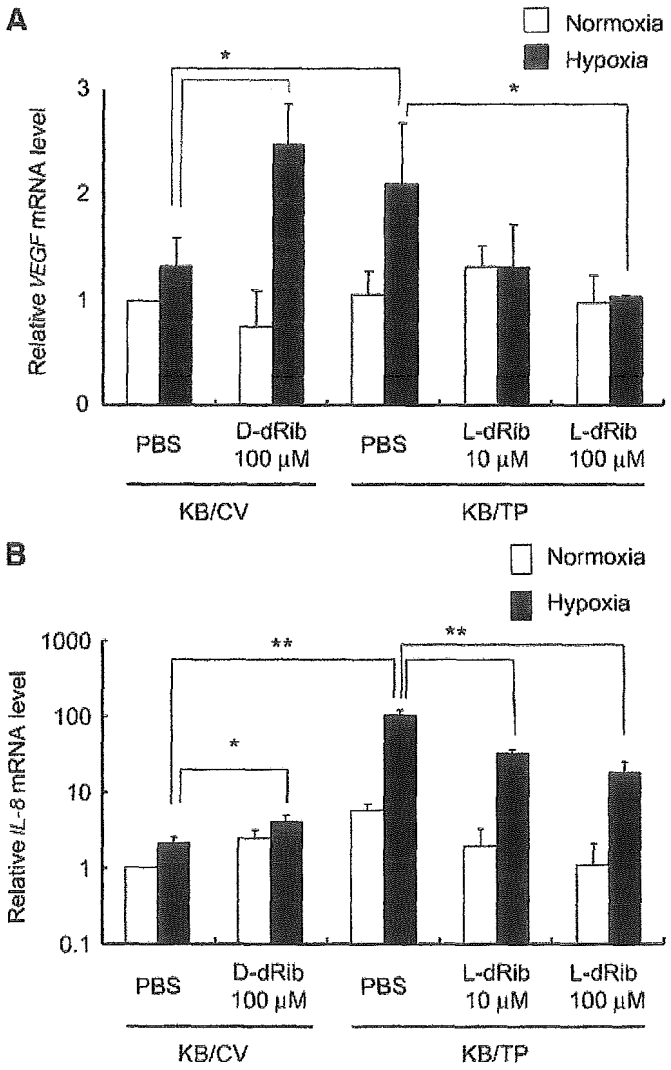

Fig. 6. The effects of D-dRib and L-dRib on the expression of angiogenic factors in cultured KB cells. KB/TP or KB/CV were cultured in serum-starved medium with or without 100 μM D-dRib (*D-dRib 100*), 10 μM L-dRib (*L-dRib 10*), 100 μM L-dRib (*L-dRib 100*), or PBS under normoxic (*open columns*) or hypoxic (*closed columns*) conditions for 48 h as indicated. Relative expression levels of *VEGF* (*A*) and *IL-8* (*B*) mRNA were measured using Real-time PCR expression of the *GAPDH* gene was used to normalize the values of *VEGF* and *IL-8*. Each column and bar represents the mean ± SD. *, $P < 0.05$. **, $P < 0.01$

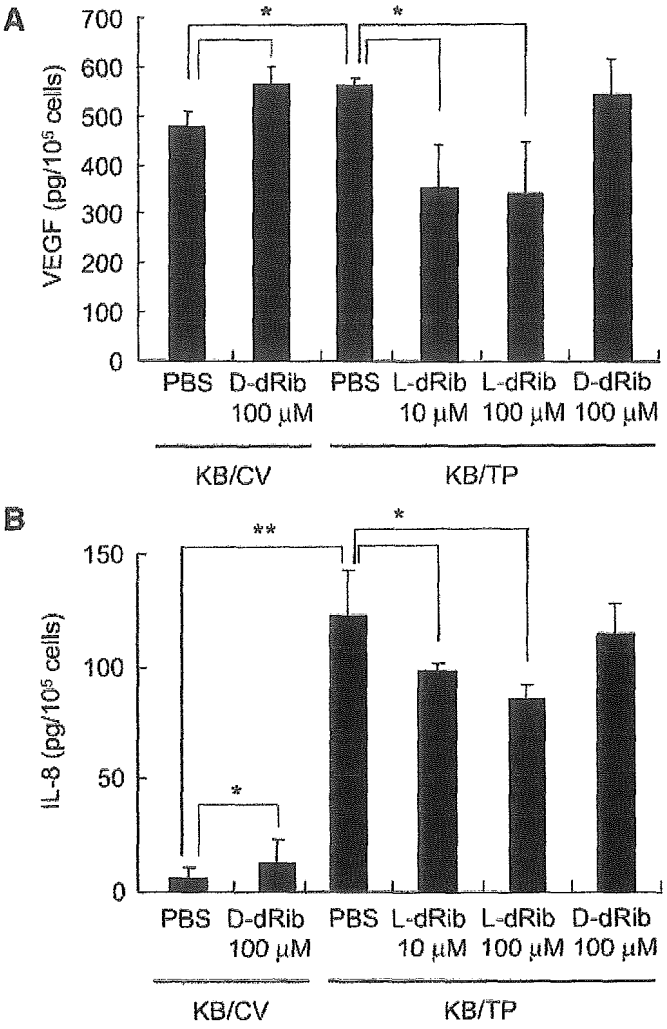

Fig. 7. Inhibition of secretion of vascular endothelial growth factor (*VEGF*) and interleukin 8 (*IL-8*) proteins from KB cells by L-dRib. *KB/TP* or *KB/CV* were cultured in serum-starved medium with or without 100 μM D-dRib (*D-dRib 100*), 10 μM L-dRib (*L-dRib 10*), 100 μM L-dRib (*L-dRib 100*) or PBS under hypoxic conditions for 48 h as indicated. VEGF (*A*) and IL-8 (*B*) protein levels were measured using an ELISA assay. Each *column* and *bar* represents the mean ± SD. *, $P < 0.05$. **, $P < 0.01$.

More importantly, treatment of KB/TP cells under hypoxic conditions with L-dRib led to a reduction in secreted protein levels of both VEGF and IL-8 (Fig. 7). Thus, inhibition of the mRNA levels for VEGF and IL-8 by L-dRib is reflected in the secreted levels of these proteins.

DISCUSSION

TP is implicated in tumor angiogenesis and metastasis (30–32). TP-mediated angiogenesis, tumor growth, and metastasis could also be inhibited by direct inhibition of TP activity by TP inhibitor (25). However, direct inhibition of TP activity by inhibitors of TP may increase plasma thymidine levels thereby causing pathological side effects (33). Thus, inhibition of D-dRib, a downstream mediator of TP function, by L-dRib will probably prove to be less toxic in a clinical setting than direct inhibition of TP activity.

L-dRib, a stereoisomer of D-dRib that has been shown to inhibit the functions of D-dRib (18), was tested for inhibition of angiogenesis and metastasis in two different mouse models in this study. In both models L-dRib inhibited angiogenesis and suppressed metastasis of tumor cells overexpressing TP. Thus, L-dRib may be an efficient antimeta-

static compound. Metastatic nodules on the surface of intestines in mice bearing s.c. KB/TP tumors were more sensitive to L-dRib than to tegafur ($P < 0.05$). Whereas the antimetastatic effects of tegafur may have been mediated by cytotoxicity (34), L-dRib at the doses used (20 mg/kg/day, 52 days) was not cytotoxic for animals. We also injected L-dRib (200 mg/kg/day) into abdominal cavities of mice for 21 days. No weight loss and no abnormal change in the organs were found (data not shown). *In vitro* experiments, the proliferation of both KB/TP and KB/CV cells was not affected when the cells were incubated in the presence of 100 μ M L-dRib for 48 and 72 h under hypoxic and also normoxic conditions (data not shown). These data suggest that L-dRib specifically inhibited TP-induced pro-metastatic effects.

The ability of L-dRib to decrease angiogenesis as well to increase the proportion of apoptotic cells in the KB/TP metastatic nodules is most likely attributable to an inhibition of TP and D-dRib pathways. We have previously demonstrated that D-dRib induces chemotaxis and tubular formation of bovine aortic endothelial cells and that these functions of D-dRib are inhibited by L-dRib (18). L-dRib was also able to suppress the prevention of hypoxia-induced apoptosis in human leukemia HL-60 cells mediated by D-dRib (19). Suppression of the enhanced levels of VEGF and IL-8 observed in KB/TP cells by L-dRib that we observed in this study was also consistent with the inhibition of TP and D-dRib pathways by L-dRib. TP has been shown to promote the secretion of angiogenic molecules such as VEGF, IL-8, and matrix metalloproteinase-1 in TP-overexpressing carcinoma cells (35). We showed that D-dRib increased the expression levels of VEGF and IL-8 in TP-negative KB/CV cells and that the expression levels of VEGF and IL-8 in KB/TP cells overexpressing TP were higher than those in KB/CV cells. These findings are also consistent with a previous report that VEGF and IL-8 are induced in TP-expressing tumor cells after the addition of thymidine (35). VEGF is angiogenic, and IL-8 not only regulates vascular endothelial cells growth, but also directly enhances matrix metalloproteinase production and the invasiveness of endothelial and tumor cells (36, 37). Although VEGF and IL-8 reportedly affected migration of various cell lines, further study is needed to confirm that L-dRib affected the invasiveness of the cells by decreasing the expression of VEGF and IL-8.

The role of oxygen in the TP and D-dRib-induced effects on VEGF and IL-8 is unclear. VEGF and IL-8 protein secretion levels are more effectively induced by hypoxia than normoxic conditions in KB/TP cells. D-dRib may be more effectively used as energy under hypoxic than normoxic conditions in tumor cells. However, the 18-fold higher induction of IL-8 under hypoxic conditions in KB/TP cells compared with control KB/CV cells cannot be explained solely by elevated levels of D-dRib. This suggests that other mechanisms for the induction of IL-8 in TP-expressing cells may exist under hypoxic conditions. Further study is needed to know whether the other degradation product(s) of thymidine by TP preferentially induce(s) IL-8.

Although L-dRib appears to modulate its effects by inhibition of D-dRib, modulated signaling pathways involved have not yet been fully elucidated. D-dRib has been implicated in a number of signaling pathways including apoptosis and integrin signaling pathways (19, 38). Because D-dRib (39), but not L-dRib (30), can enter glycolysis and provide an energy source (40), D-dRib may be an important energy source under hypoxic conditions. L-dRib inhibition of D-dRib entry into glycolsyis could, thus, be detrimental to tumor growth under hypoxic conditions. Recent evidence suggests that D-dRib affects endothelial cell migration via activation of integrin downstream signaling pathways (38). Thus, L-dRib may block either the association of D-dRib to the cell surface receptor and/or D-dRib-induced downstream signaling pathways in endothelial cells.

Although the complex pathways involved in D-dRib-modulated

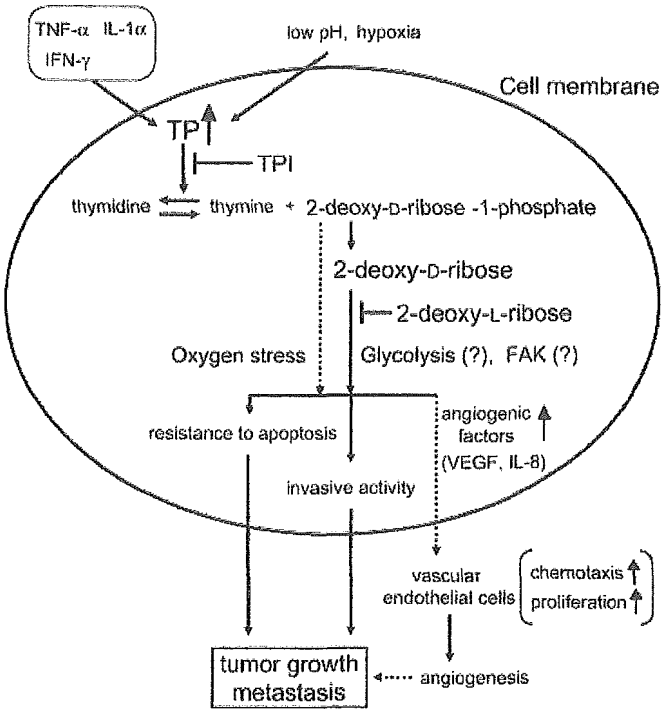

Fig. 8. Schematic representation of the role of thymidine phosphorylase (TP) and D-dRib in tumorigenesis and its inhibition by L-dRib. The expression of TP is induced by cytokines, hypoxia, or low pH in various tumor cells. TP catalyzes the reversible conversion of thymidine to thymine and 2-deoxy-D-ribose-1-phosphate D-dRib is produced by dephosphorylation of 2-deoxy-D-ribose-1-phosphate. D-dRib is a downstream mediator of TP and confers resistance to hypoxia-induced apoptosis, enhances chemotaxis of vascular endothelial cells, and causes angiogenesis and metastasis. 2-Deoxy-L-ribose can suppress these various biological effects of D-dRib, leading to an inhibition of tumorigenesis.

effects remain to be fully elucidated, it is clear from this study that o.p. administration of L-dRib can suppress TP-mediated metastasis. This is the first demonstration that L-dRib may be useful as an antimetastatic agent for the various solid tumors overexpressing TP. In future studies, combination chemotherapy of L-dRib with other anticancer or antiangiogenic agents may be even more effective in the suppression of the growth and metastasis of tumors overexpressing TP (Fig. 8).

In conclusion, L-dRib inhibits metastasis probably by suppressing TP-stimulated expression of angiogenic factors such as *VEGF* and *IL-8*, and L-dRib may prove to be a more efficient and less toxic agent than currently available drugs for the inhibition of metastasis of TP-expressing tumors.

REFERENCES

1. Folkman, J. Tumor angiogenesis: therapeutic implications. N. Engl. J. Med., *285:* 1182–1186, 1971.
2. Senger, D. R., Perruzzi, C. A., Feder, J., and Dvorak, H. F. A highly conserved vascular permeability factor secreted by a variety of human and rodent tumor cell lines. Cancer Res., *46:* 5629–5632, 1986.
3. Schweigerer, L., Neufeld, G., Friedman, J., Abraham, J. A., Fiddes, J. C., and Gospodarowicz, D. Capillary endothelial cells express basic fibroblast growth factor, a mitogen that promotes their own growth. Nature (Lond.), *325:* 257–259, 1987.
4. Rappolee, D. A., Mark, D., Banda, M. J., and Werb, Z. Wound macrophages express TGF-α and other growth factors *in vivo*: analysis by mRNA phenotyping. Science (Wash. DC), *241:* 708–712, 1988.
5. Grant, D. S., Kleinman, H. K., Goldberg, I. D., Bhargava, M. M., Nickoloff, B. J., Kinsella, J. L., Polverini, P., and Rosen, E. M. Scatter factor induces blood vessel formation *in vivo*. Proc. Natl. Acad. Sci. USA, *90:* 1937–1941, 1993.
6. Folkman, J. Angiogenesis in cancer, vascular, rheumatoid and other disease. Nat. Med., *1:* 27–31, 1995.
7. Hanahan, D., and Folkman, J. Patterns and emerging mechanisms of the angiogenic switch during tumorigenesis. Cell, *86:* 353–364, 1996.
8. Folkman, J. Anti-angiogenesis: new concept for therapy of solid tumors. Ann. Surg., *175:* 409–416, 1972.

9. Furukawa, T., Yoshimura, A., Sumizawa, T., Haraguchi, M., Akiyama, S., Fukui, K., Ishizawa, M., and Yamada, Y. Angiogenic factor. Nature (Lond.), *356:* 668, 1992.
10. Haraguchi, M., Miyadera, K., Uemura, K., Sumizawa, T., Furukawa, T., Yamada, K., Akiyama, S., and Yamada, Y. Angiogenic activity of enzymes. Nature (Lond.), *368:* 198, 1994.
11. Matsushita, S., Nitanda, T., Furukawa, T., Sumizawa, T., Tani, A., Nishimoto, K., Akiba, S., Miyadera, K., Fukushima, M., Yamada, Y., Yoshida, H., Kanzaki, T., and Akiyama, S. The effect of a thymidine phosphorylase inhibitor on angiogenesis and apoptosis in tumors. Cancer Res., *59:* 1911–1916, 1999.
12. Takebayashi, Y., Akiyama, S., Akiba, S., Yamada, K., Miyadera, K., Sumizawa, T., Yamada, Y., Murata, F., and Aikou, T. Clinicopathologic and prognostic significance of an angiogenic factor, thymidine phosphorylase, in human colorectal carcinoma. J. Natl. Cancer Inst., *88:* 1110–1117, 1996.
13. Yonenaga, F., Takasaki, T., Ohi, Y., Sagara, Y., Akiba, S., Yoshinaka, H., Aikou, T., Miyadera, K., Akiyama, S., and Yoshida, H. The expression of thymidine phosphorylase/platelet-derived endothelial cell growth factor is correlated to angiogenesis in breast cancer. Pathol. Int., *48:* 850–856, 1998.
14. Shimaoka, S., Matsushita, S., Nitanda, T., Matsuda, A., Nioh, T., Suenaga, T., Nishimata, Y., Akiba, S., Akiyama, S., and Nishimata, H. The role of thymidine phosphorylase expression in the invasiveness of gastric carcinoma. Cancer (Phila.), *88:* 2220–2227, 2000.
15. Giatromanolaki, A., Sivridis, E., Simopoulos, C., Polychronidis, A., Gatter, K. C., Harris, A. L., and Koukourakis, M. I. Thymidine phosphorylase expression in gallbladder adenocarcinomas. Int. J. Surg. Pathol., *10:* 181–188, 2002.
16. Kitazono, M., Takebayashi, Y., Ishitsuka, K., Takao, S., Tani, A., Furukawa, T., Miyadera, K., Yamada, Y., Aikou, T., and Akiyama, S. Prevention of hypoxia-induced apoptosis by the angiogenic factor thymidine phosphorylase. Biochem. Biophys. Res. Commun., *253:* 797–803, 1998.
17. Miyadera, K., Sumizawa, T., Haraguchi, M., Yoshida, H., Konstanty, W., Yamada, Y., and Akiyama, S. Role of thymidine phosphorylase activity in the angiogenic effect of platelet derived endothelial cell growth factor/thymidine phosphorylase. Cancer Res., *55:* 1687–1690, 1995.
18. Uchimiya, H., Furukawa, T., Okamoto, M., Nakajima, Y., Matsushita, S., Ikeda, R., Gotanda, T., Haraguchi, M., Sumizawa, T., Ono, M., Kuwano, M., Kanzaki, T., and Akiyama, S. Suppression of thymidine phosphorylase-mediated angiogenesis and tumor growth by 2-deoxy-L-ribose. Cancer Res., *62:* 2834–2839, 2002.
19. Ikeda, R., Furukawa, T., Kitazono, M., Ishitsuka, K., Okumura, H., Tani, A., Sumizawa, T., Haraguchi, M., Komatsu, M., Uchimiya, H., Ren, X. Q., Motoya, T., Motoya, T., Yamada, K., and Akiyama, S. Molecular basis for the inhibition of hypoxia-induced apoptosis by 2-deoxy-D-ribose. Biochem. Biophys. Res. Commun., *291:* 806–812, 2002.
20. Klein, R. S., Lenzi, M., Lim, T. H., Hotchkiss, K. A., Wilson, P., and Schwartz, E. L. Novel 6-substituted uracil analogs as inhibitors of the angiogenic actions of thymidine phosphorylase. Biochem. Pharmacol., *62:* 1257–1263, 2001.
21. Nishino, I., Spinazzola, A., and Hirano, M. Thymidine phosphorylase gene mutations in MNGIE, a human mitochondrial disorder. Science (Wash. DC), *283:* 689–692, 1999.
22. Nishino, I., Spinazzola, A., Papadimitriou, A., Hammans, S., Steiner, I., Hahn, C. D., Connolly, A. M., Verloes, A., Guimaraes, J., Maillard, I., Hamano, H., Donati, M. A., Semrad, C. E., Russell, J. A., Andreu, A. L., Hadjigeorgiou, G. M., Vu, T. H., Tadesse, S., Nygaard, T. G., Nonaka, I., Hirano, I., Bonilla, E., Rowland, L. P., DiMauro, S., and Hirano, M. Mitochondrial neurogastrointestinal encephalomyopathy: an autosomal recessive disorder due to thymidine phosphorylase mutations. Ann. Neurol., *47:* 792–800, 2000.
23. Verweij, J. Rational design of new tumor activated cytotoxic agents. Oncology, *57:* 9–15, 1999.
24. Haraguchi, M., Furukawa, T., Sumizawa, T., and Akiyama, S. Sensitivity of human KB cells expressing platelet-derived endothelial cell growth factor to pyrimidine antimetabolites. Cancer Res., *53:* 5680–5682, 1993.
25. Takao, S., Akiyama, S., Nakajo, A., Yoh, H., Kitazono, M., Natsugoe, S., Miyadera, K., Fukushima, M., Yamada, Y., and Aikou, T. Suppression of metastasis by thymidine phosphorylase inhibitor. Cancer Res., *60:* 5345–5648, 2000.
26. Potter, H., Weir, L., and Leder, P. Enhancer-dependent expression of human κ immunoglobulin genes introduced into mouse pre-B lymphocytes by electroporation. Proc. Natl. Acad. Sci. USA, *81:* 7161–7165, 1984.
27. Takebayashi, Y., Yamada, K., Miyadera, K., Sumizawa, T., Furukawa, T., Kinoshita, F., Aoki, D., Okumura, H., Yamada, Y., Akiyama, S., and Aikou, T. The activity and expression of thymidine phosphorylase in human solid tumors. Eur. J. Cancer, *32:* 1227–1232, 1996.
28. Drixler, T. A., Rinkes, I. H., Ritchie, E. D., van Vroonhoven, T. J., Gebbink, M. F., and Voest, E. E. Continuous administration of angiostatin inhibits accelerated growth of colorectal liver metastases after partial hepatectomy. Cancer Res., *60:* 1761–1765, 2000.
29. Guba, M., von Breitenbuch, P., Steinbauer, M., Koehl, G., Flegel, S., Hornung, M., Bruns, C. J., Zuelke, C., Farkas, S., Anthuber, M., Jauch, K. W., and Geissler, E. K. Rapamycin inhibits primary and metastatic tumor growth by antiangiogenesis: involvement of vascular endothelial growth factor. Nat. Med., *8:* 128–135, 2002.
30. Brown, N. S., and Bicknell, R. Thymidine phosphorylase, 2-deoxy-D-ribose and angiogenesis. Biochem. J., *334:* 1–8, 1998.
31. Ueda, M., Terai, Y., Kumagai, K., Ueki, K., Kanemura, M., and Ueki, M. Correlation between thymidine phosphorylase expression and invasion phenotype in cervical carcinoma cells. Int. J. Cancer, *91:* 778–782, 2001.
32. Muro, H., Waguri-Nagaya, Y., Mukofujiwara, Y., Iwahashi, T., Otsuka, T., Matsui, N., Moriyama, A., Asai, K., and Kato, T. Autocrine induction of gliostatin/platelet-derived endothelial cell growth factor (GLS/PD-ECGF) and GLS-induced expression of matrix metalloproteinases in rheumatoid arthritis synoviocytes. Rheumatology (Oxford), *38:* 1195–1202, 1999.
33. Haraguchi, M., Tsujimoto, H., Fukushima, M., Higuchi, I., Kuribayashi, H., Utsumi, H., Nakayama, A., Hashizume, Y., Hirato, J., Yoshida, H., Hara, H., Hamano, S., Kawaguchi, H., Furukawa, T., Miyazono, K., Ishikawa, F., Toyoshima, H., Kaname, T., Komatsu, M., Chen, Z. S., Gotanda, T., Tachiwada, T., Sumizawa, T., Miyadera, K., Osame, M., Yoshida, H., Noda, T., Yamada, Y., and Akiyama, S. Targeted deletion of both thymidine phosphorylase and uridine phosphorylase and consequent disorders in mice. Mol. Cell. Biol., *22:* 5212–5221, 2002.
34. Tuchman, M., Stoeckeler, J. S., Kiang, D. T., O'Dea, R. F., Ramnaraine, M. L., and Mirkin, B. L. Familial pyrimidinemia and pyrimidinuria associated with severe fluorouracil toxicity. N. Engl. J. Med., *313:* 245–249, 1985.
35. Brown, N. S., Jones, A., Fujiyama, C., Harris, A. L., and Bicknell, R. Thymidine phosphorylase induces carcinoma cell oxidative stress and promotes secretion of angiogenic factors. Cancer Res., *60:* 6298–6302, 2000.
36. Li, A., Dubey, S., Varney, M. L., Dave, B. J., and Singh, R. K. IL-8 directly enhanced endothelial cell survival, proliferation, and matrix metalloproteinases production and regulated angiogenesis. J. Immunol., *170:* 3369–3376, 2003.
37. Ramjeesingh, R., Leung, R., and Siu, C. H. Interleukin-8 secreted by endothelial cells induces chemotaxis of melanoma cells through the chemokine receptor CXCR1. FASEB J., *17:* 1292–1294, 2003.
38. Hotchkiss, K. A., Ashton, A. W., and Schwartz, E. L. Thymidine phosphorylase and 2-deoxyribose stimulate human endothelial cell migration by specific activation of the integrins $\alpha_5\beta_1$ and $\alpha_V\beta_3$. J. Biol. Chem., *278:* 19272–19279, 2003.
39. Vogel, T., Blake, D. A., Whikehart, D. R., Guo, N. H., Zabrenetzky, V. S., and Roberts, D. D. Specific simple sugars promote chemotaxis and chemokinesis of corneal endothelial cells. J. Cell Physiol., *157:* 359–366, 1993.
40. Kim, C. H., and Kho, Y. H. Domain structure and multiplicity of raw-starch-digesting amylase from Bacillus circulans: extensive proteolysis with proteinase K, endopeptidase Glu-C and thermolysin. Biochim. Biophys. Acta, *1202:* 200–206, 1993.

Histopathology 2003, **42**, 541–545

Expression of maspin is up-regulated during the progression of mammary ductal carcinoma

Y Umekita & H Yoshida
Department of Pathology, Faculty of Medicine, Kagoshima University, Kagoshima, Japan

Date of submission 5 August 2002
Accepted for publication 26 November 2002

Umekita Y & Yoshida H
(2003) *Histopathology* **42**, 541–545

Expression of maspin is up-regulated during the progression of mammary ductal carcinoma

Aims: The tumour suppressor gene *maspin* is reported to inhibit the motility, invasiveness and metastasis of breast cancer cells. Maspin is expressed in normal mammary myoepithelial cells but is down-regulated during the progression of ductal carcinoma. However, we recently reported that maspin expression was frequently observed in invasive ductal carcinoma (IDC) with an aggressive phenotype, and it was a strong indicator of a poor prognosis. To our knowledge, to date, there has been no report investigating maspin expression in a large series of ductal carcinoma in situ (DCIS).

Methods and results: To clarify whether there is down-regulation during the progression of ductal carcinoma, we immunohistochemically investigated the expression of maspin in 145 DCIS, 92 invasive ductal carcinomas with a predominant intraductal component as well as 94 usual ductal hyperplasias and 27 atypical ductal hyperplasias. The expression of maspin in carcinoma cells was observed in 9.6% (14 of 145) of DCIS and 18.5% (17 of 92) of IDC with a predominant intraductal components. It significantly correlated with larger tumour size ($P = 0.013$; $P = 0.042$), higher histological grade ($P = 0.015$; $P = 0.0003$) and the presence of comedo-necrosis ($P = 0.000005$; $P = 0.0074$) in DCIS and IDC with a predominant intraductal components, respectively. In epithelial cells, the expression of maspin was observed in only one case of usual ductal hyperplasia, and all cases of atypical ductal hyperplasia were negative.

Conclusions: These results and our previous investigation in which 27.4% of IDC were positive for maspin suggest that the expression of maspin in epithelial cells could be up-regulated during the progression of ductal carcinoma, and that it could be correlated with the acquisition of an aggressive phenotype.

Keywords: maspin, ductal carcinoma in situ, immunohistochemistry

Abbreviations: DCIS, ductal carcinoma in situ; IDC, invasive ductal carcinoma

Introduction

Maspin is a unique member of the serpin (serine protease inhibitor) superfamily.[1] The *maspin* gene was originally isolated from normal human mammary epithelial cells by subtractive hybridization, and it has been shown to have tumour suppressor activity attributable to the inhibition of breast cancer cell motility, invasion and metastases.[2–4] According to the first immunohistochemical study of 12 invasive breast carcinomas, 11 regional lymph nodes and two pleural effusions containing metastatic breast cancer, the maspin protein was expressed in normal human mammary myoepithelial cells but was down-regulated during cancer progression.[1] Recently, Maass *et al.* reported that a significant stepwise decrease in maspin expression occurred in the sequence of ductal carcinoma in situ (DCIS)–invasive cancer–lymph node metastasis using 12 DCIS, 128 invasive ductal carcinomas (IDC), 65 lymph nodes and 22 cases of fibrocystic change.[5] However, we recently reported that maspin expression was frequently observed in IDC with an aggressive phenotype, and was a strong predictor of a

Address for correspondence: Yoshihisa Umekita MD, Department of Pathology, Faculty of Medicine, Kagoshima University, 8-35-1, Sakuragaoka, Kagoshima 890-8520, Japan.
e-mail: umekita@m2.kufm.kagoshima-u.ac.jp